Res Mechanica **31** (1991) 399–453

Creep of Dispersion Strengthened Materials: A Critical Assessment

E. Arzt

Universität Stuttgart, Institut für Metallkunde, and Max-Planck-Institut für Metallforschung, Seestraße 92, D7000 Stuttgart 1, FRG

(Received 15 September 1988)

ABSTRACT

Experimental investigations into the creep behaviour of dispersion-strengthened materials, with emphasis on dislocation creep in nickel and aluminium base alloys, are reviewed. Points of interest are the 'anomalously' high stress dependence of the creep rates, the role of grain boundaries, and the loss of strength at high temperatures. Theoretical attempts to explain the creep behaviour in terms of interactions between dislocations and dispersoid particles are extensively discussed. It is concluded that recent models based on an attractive dispersoid–dislocation interaction bear great promise for explaining some phenomena which are not understood on the basis of more classical dislocation climb theories. For the purpose of creep data extrapolation, it follows that the 'threshold stress' concept is only an approximation which must not be used uncritically. Further considerations regarding models for the effects of grain boundaries on deformation and fracture are briefly presented. The importance of a theoretical understanding of dispersoid effects for designing optimum alloys is stressed, and areas for further work are outlined.

NOTATION

A, A', B, C	Dimensionless constants
$a_p D_p$	Cross-section of dislocation core times its diffusivity
b	Burgers vector of a lattice dislocation
d	Edge length of cuboidal dispersoids (Fig. 16(b))

Res Mechanica 0143-0084/91/$03·50
Printed in Northern Ireland

D_V	Volume diffusivity
E	Young's modulus
f_V	Volume fraction of dispersoids
G	Shear modulus
k	Relaxation factor (eqn (13))
k_B	Boltzmann's constant
l	Mean planar dispersoid spacing
n	Stress exponent (see eqn (1))
Q	Activation energy
r	Radius of spherical dispersoid particles
R	Grain aspect ratio (abbreviated GAR in text) (eqn (15))
T	Absolute temperature
Γ	Specific line energy of a lattice dislocation
δD_b	Grain boundary thickness times its diffusivity
$\dot{\varepsilon}$	Strain rate
ρ	Mobile dislocation density
σ	Stress
σ_0	'Threshold stress' (eqn. (4))
σ_d	Detachment stress (eqn (13))
σ_{Or}	Orowan stress (eqn (7))
σ_{th}	Mechanistic 'threshold stress' (eqns (9) and (11))
τ	Shear stress
τ_{Or}	Orowan stress in shear
Ω	Atomic volume

1 INTRODUCTION

The incorporation of fine stable dispersoid particles in a metallic matrix can raise the high temperature capability of a material substantially. Such dispersion strengthened alloys generally retain useful strength up to a relatively high fraction of their melting points where other strengthening mechanisms, e.g. precipitation hardening or solid solution strengthening, rapidly lose their effectiveness. Dispersion strengthening has been applied to many alloy systems, most notably to Ni-base, Fe-base, Al, W, Pt, Pb and Cu alloys. An attractive feature of this mechanism is that it can be superimposed on other hardening mechanisms: the prime example is oxide dispersion strengthened ('ODS') superalloys which combine excellent high temperature strength (due to the dispersoids) with good intermediate strength (due to ordered precipitates). Such alloys are promising candidates for applications in advanced gas turbines and combustion engines.

In order to be useful at high temperatures, one of the requirements for dispersoid particles is thermodynamic stability. Therefore high-melting point ceramic particles, whose constituents have low solubility and diffusivity in the matrix, are usually chosen. Such dispersoid particles can be introduced in a metallic matrix by coprecipitation, internal oxidation and powder metallurgical techniques. In the late 1940s Al_2O_3-strengthened aluminium was developed by Irmann[1] and van Zeerleder.[2] This material, which is known by its acronym 'SAP' (Sintered Aluminium Powder), was produced by milling Al powder under oxidizing conditions and subsequent compaction by extrusion. Low ductility, poor reproducibility of properties and high price, however, prevented widespread application of SAP. The breakthrough for powder-metallurgical methods came with 'Mechanical Alloying', invented by Benjamin,[3] which allowed much more homogeneous dispersoid distributions to be produced and is now widely used. The processing involves a high-energy milling of the starting powders with the dispersoid particles, followed by consolidation and thermomechanical processing (for a recent review see Singer and Arzt[4]). In a similar process, termed 'Reaction Milling', Jangg and Kutner[5] and Jangg[6] formed dispersoid particles by reaction of milling additions with the powder. Typical dispersoid microstructures of two materials which are currently being studied extensively are shown in Fig. 1.

The strength advantage of dispersion strengthened materials over dispersoid free alloys increases at high temperatures and low strain rates. The creep behaviour of such alloys is therefore of particular interest, both from a technological and a scientific point of view, and has been studied in detail. The purpose of this paper is to review the experimental and theoretical investigations of the effects of dispersoid particles on creep behaviour. The emphasis will be on steady-state or secondary creep behaviour, with some reference to creep fracture. In the context of this paper dispersoids are defined as incoherent particles in low volume fractions (generally less than 10%), formed by means other than precipitation, although in some cases the dividing line *vis-à-vis* precipitates is difficult to draw.

In view of the extensive literature in this field, it would be a formidable task to attempt to do justice to all investigators. The reader is therefore also referred to earlier reviews of the subject, most notably by Ansell[7], Ashby,[8] Gibeling and Nix,[9] Brown,[10,11] Bilde-Sørensen,[12] Cadek and Ilschner[13] and Blum and Reppich[14] for developments in theoretical understanding; to Sellars and Petkovic-Luton,[15] Lin and Sherby[16] and Martin[17] for more general aspects; and to Benjamin,[3] Morall,[18] Singer and Gessinger[19] and Singer and Arzt[4] for processing

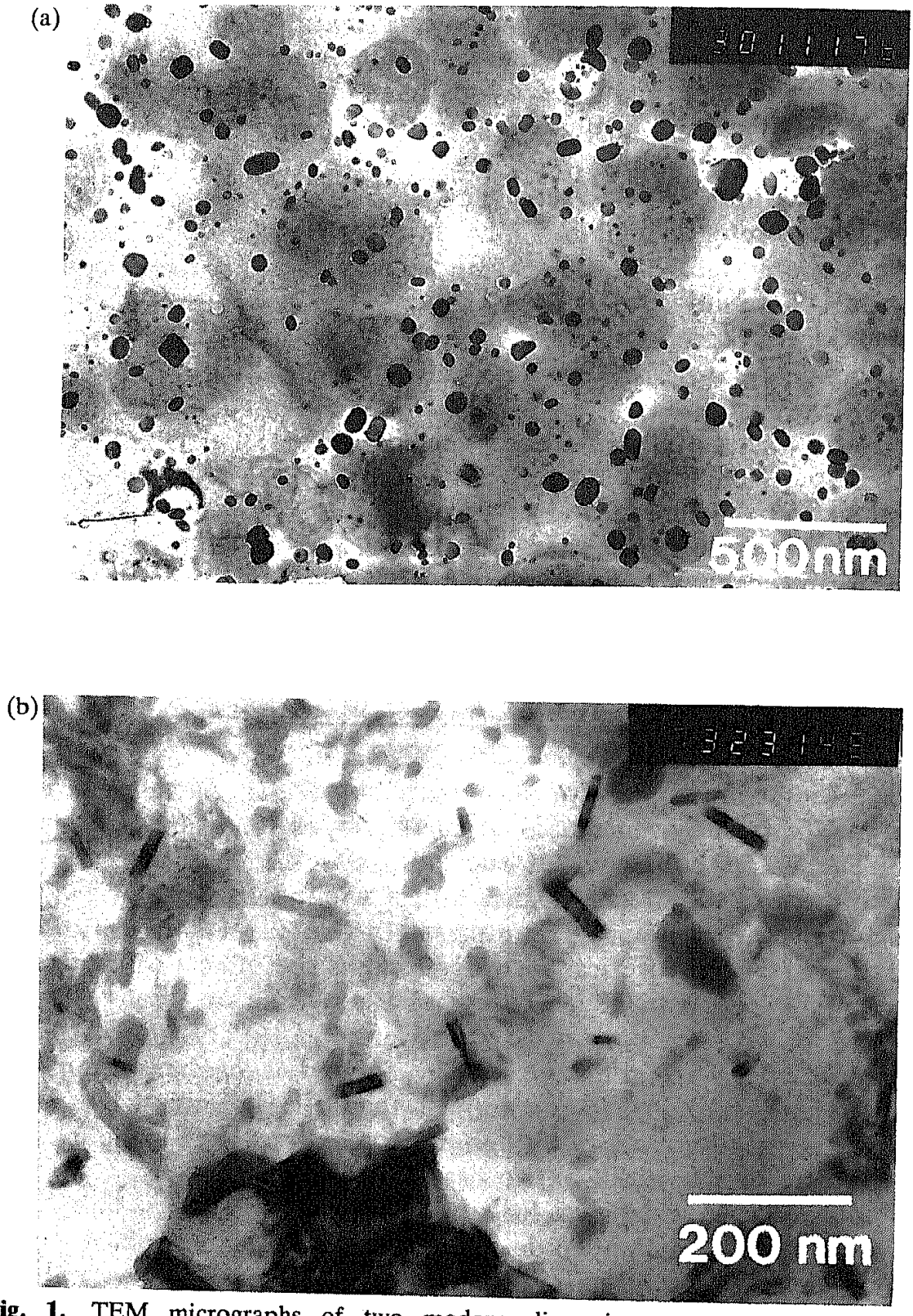

Fig. 1. TEM micrographs of two modern dispersion strengthened engineering materials: (a) the nickel base superalloy Inconel MA 6000 with Y_2O_3 dispersoids (small dark particles) and γ' precipitates (larger shadows in the background), produced by Mechanical Alloying (from Ref. 4); (b) the aluminium alloy AlC2 with Al_4C_3 (dark platelets) and Al_2O_3 dispersoids (light equiaxed particles), produced by Reaction Milling (from Refs 65 and 66).

and properties. By focusing on more recent developments, the present paper aims to update and complement these earlier reviews.

2 PHENOMENOLOGY OF CREEP IN DISPERSION STRENGTHENED MATERIALS

In this section the relevant experimental observations relating to creep in dispersion-strengthened engineering materials are presented (Section 2.1). Then an attempt is made in Section 2.2 to summarize the phenomenological trends in order to set the scene for a description of mechanistic models in the subsequent Section 3. Finally it is demonstrated in Section 2.3 how the popular 'threshold stress' concept can be used to formally rationalize some aspects of the creep behaviour in a phenomenological way, i.e. without providing a mechanistic justification.

2.1 Experimental investigations

Numerous investigations with dispersion strengthened materials were carried out in the 1960s and 1970s when thoria-dispersed nickel (TD-Ni) and Al_2O_3-strengthened aluminium (SAP) attracted great practical interest. The activity in this field was rekindled by the advent of new dispersion strengthened Ni, Fe and Al alloys produced by the 'mechanical alloying' process in the 1970s and 1980s. This section describes the salient features of experimental investigations into the creep behaviour, focusing on nickel and aluminium-base alloys. Compositions and further details of the alloys discussed below are given in Table 1.

2.1.1 *Nickel alloys*

The systematic studies of dispersion strengthening at high temperatures in nickel alloys commence with the pioneering work of Wilcox and Clauer[20–23] on thoria-dispersed (TD) nickel. As neither single crystal material nor highly elongated grain structures were available at the time, these investigations concentrated on the effects of grain boundaries and grain shape. One of the most important results was the conclusion that an elongated grain shape can exhibit better creep strength than a coarser but equiaxed grains structure. Kane and Ebert[24] were the first to experimentally confirm the superior creep strength of TD–NiCr single crystals.

First conclusions about the creep mechanisms in dispersion strength-

TABLE 1
Alloy Compositions and Typical Microstructural Parameters

System	*Designation*	*Composition (wt%)*	*Dispersoid size (mm)*	*Vol%*	*Grain size (GAR)*	*Ref.*
$Ni–ThO_2$	TD–Ni	$Ni–ThO_2$	37	2	10×1 μm, (10)	20–23
$NiCr–ThO_2$	TD–NiCr	$Ni–20Cr–ThO_2$	10–15	2	single crystal 30×70 and 100×300 μm	24–26,16
$NiCr–Y_2O_3$	Inconel MA 754	$Ni–20{\cdot}5Cr–0{\cdot}3Al–0{\cdot}35Ti–0{\cdot}13Fe + Y_2O_3$	13	2·5	~mm (10)	28–31
$NiCrAlTi–Y_2O_3$	Inconel MA 6000	$Ni–15{\cdot}5Cr–4{\cdot}5Al–2{\cdot}5Ti–4W–2Mo–2Ta–Y_2O_3$	33	2·5	10 mm (10–60)	4, 30, 32–40
$Al–Al_2O_3$ (SAP)	SAP	$Al–0{\cdot}19...0{\cdot}92Al_2O_3$	20–50	0·2–0·9	mm (≤40)	54–57
Al–C,O	—	$Al–0{\cdot}53C–1{\cdot}5O–0{\cdot}9Fe$	14		μm	58
AlMg–C,O	IN 9051	Al–3·9 Mg–0·39 C–1·85 O–0·098 Fe	14		μm	58
AlMg–C,O	IN 9052	Al–4 Mg–1·1 C–0·8 O	10		0·5μm	59, 60
AlCuMg-C,O	IN 9021	Al–4 Cu–1·5 Mg–(C,O)	10–20	4·5	0·9μm	61, 63
Al–C,O	DISPAL		~30	0.1..8		65–69
		$Al–0{\cdot}03...2{\cdot}2C–1O–Al_4C_3–Al_2O_3$		1·4	~1 μm	
AlMg–C,O	—	$Al–4Mg–1{\cdot}42C–2{\cdot}6O–Al_4C_3–MgO$	~30	5·2,4·9	0·4 μm	65, 66
Al–O	—	$Al–Al_2O_3$	50	0·4	0·1 and 1 μm	64
AlSi–O	—	$Al–1\%Si–Al_2O_3$	60	0·4	30 μm	64
AlFeCe–C,O	—	$Al–8{\cdot}4\ Fe–3{\cdot}4Ce–Al_2O_3, Al_4C_3$	50		30 μm	71
$FeCr–Y_2O_3$	Incoloy MA 956	$Fe–20Cr–4{\cdot}51Al–0{\cdot}5Ti–0{\cdot}5Y_2O_3$	24	3	single	73
FeCr–NbC	—	$Fe–20Cr–0...0{\cdot}8\%NbC$	50	0...0·8	30 μm	74, 75
W–K	K-doped tungsten	W–68...80 ppm K	9	0·2	wire 180 μm(10–60)	76, 77

ened materials were drawn in a celebrated paper by Lund and Nix,[25] who studied the stress and temperature dependence of creep in single crystal TD–NiCr. The stress sensitivity of the creep rate increased at higher temperatures, with 'stress exponents' n getting as high as 75 (Fig. 2(a)). At very high temperatures (1200 and 1300 °C) and low creep rates, a transition to lower stress sensitivity, which the authors ascribed to the dissolution of small dispersoids, was observed. On a normalized plot of $\dot{\varepsilon}/D_V$ versus σ/E (Fig. 2(b)), the data points for different temperatures fall on a single curve, suggesting that the creep rate is essentially determined by volume diffusion. A stress level of $\sigma/E \approx 6 \times 10^{-3}$ can be identified in Fig. 2(b) below which the creep rate virtually vanishes. This stress value, termed 'threshold stress' by the authors, was found to be identical with the Orowan stress, as calculated from dispersoid parameters determined by TEM of extraction replicas. The creep strength of the alloy could be well explained by assuming that the 'threshold stress' adds linearly to the creep strength of the dispersoid-free matrix material. In a follow-up paper, Pharr and Nix[26] showed by calibration with the room-temperature yield stress that in fact the 'threshold stress' amounted to only about 60% of the Orowan stress. This is the first reliable indication that the Orowan limit is not reached during creep deformation of dispersion strengthened materials. Lund and Nix[25] also report elongations-to-failure which were up to an order of magnitude higher than for polycrystals and increased with increasing creep stress/strain rate. Failure was concluded to occur by plastic instability of the specimen. When compared with the single-crystal data, polycrystalline material (also shown in Fig. 2(b)) was considerably weaker and did not exhibit 'threshold stress' behaviour.

A remarkable grain size effect was also reported by Lin and Sherby,[16] who studied the compression creep behaviour of TD–NiCr with two different grain diameters. The coarser grain material behaved similarly to the single crystals of Lund and Nix[25] and Kane and Ebert,[24] showing increasing stress sensitivity at lower stresses. By contrast, the fine grain material exhibited only a moderate stress exponent ($n \approx 8$), which remained constant over three decades in the strain rate. (The authors also cite several examples of other polycrystalline materials having a constant stress exponent $n \approx 9$ over up to eight orders of magnitude in strain rate.) The creep rates were found to be independent of the loading direction with respect to the extrusion axis.

Since the invention of the mechanical alloying process,[3] alloys with superior high temperature strength due to an improved distribution of stable oxide particles have become available for investigations. During the development of these alloys the necessity for a well-defined grain

(a)

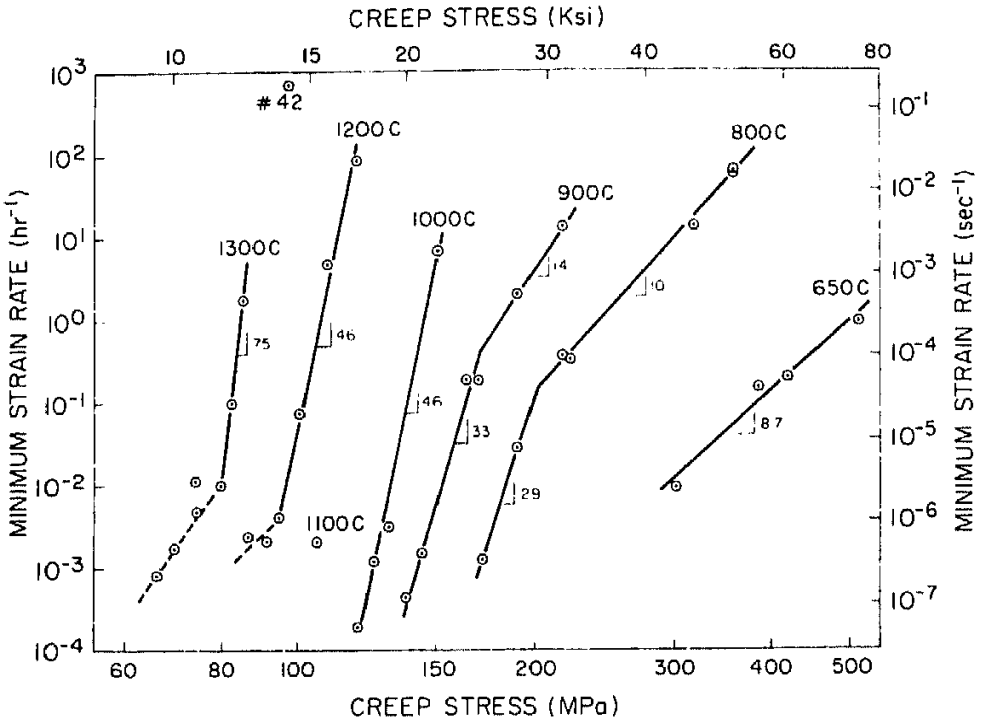

(b)

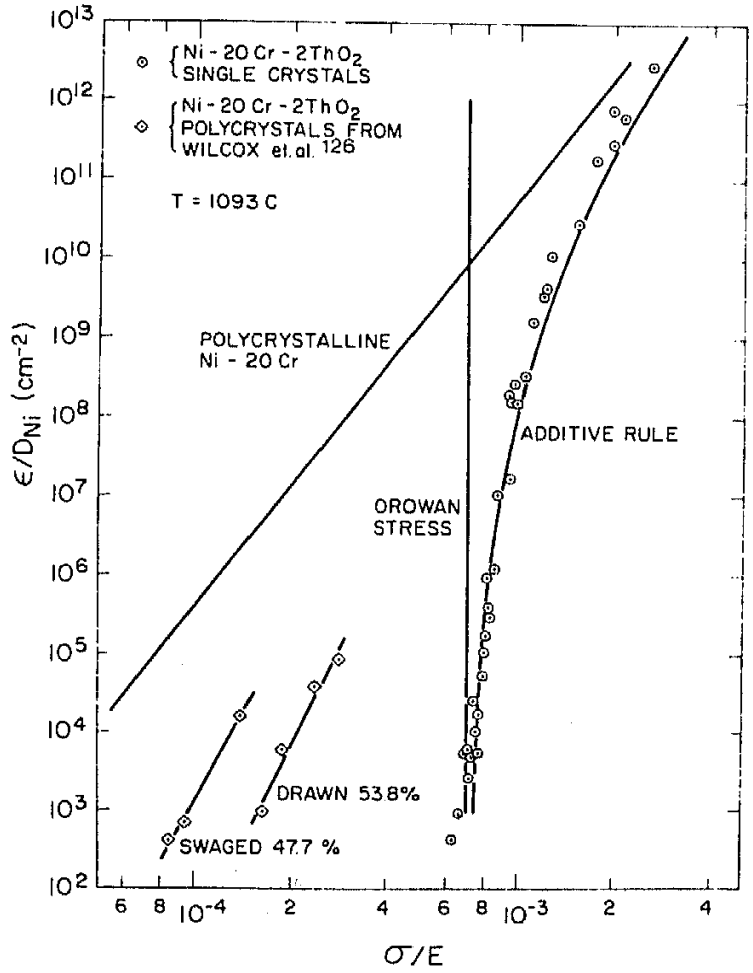

Fig. 2. Creep properties of TD–NiCr single crystals with typical 'threshold stress' behaviour (Ref. 25): (a) minimum strain rate versus applied stress; (b) normalized plot of the same data (also shown are the calculated Orowan stress, data for polycrystalline Ni–Cr and TD–NiCr material and the prediction for single crystals following addition of matrix strength and Orowan stress).

coarsening treatment was realized.[27] The resulting material consists of large grains, elongated in the extrusion direction ('fibre grain morphology'). INCONEL MA 754, a Ni–Cr solid solution with Y_2O_3 dispersoids, was found to exhibit high stress sensitivity.[28] Two different heats with varying grain structure were studied in detail by Stephens and Nix.[29] In the uniform fibre grain morphology of 'heat 1' stress exponents in the range $n \approx 40$ to 46 were found and creep fracture was transgranular at high stresses, while a lower n ($\approx$5 to 16) appeared at low stresses, associated with a transition to intergranular fracture. Isolated fine grain pockets ('heat 2') were found to reduce long-term creep strength and rupture times remarkably although the short-term strength improved (Fig. 3(a)). The authors note that a trade-off exists between long and short-term strength: the slightly higher volume fraction of dispersoids in 'heat 2', while responsible for short-term strength, seemed to make the attainment of a uniform fibre grain morphology, which is important for long-term behaviour, difficult. Also, the 'threshold concept' is found to be problematic for polycrystalline materials. When tested in the fine-grained condition,[30] this alloy again exhibits a reduced stress sensitivity, with high elongations indicative of superplasticity.[31] At low strain rates the stress exponent reverts to values similar to those in the coarse grain but the strength of the fine grain is decreased by a factor of about 5 relative to the coarse grain (Fig. 3(b)).

A superposition of solid solution strengthening, precipitation hardening and dispersion strengthening has been achieved in the ODS superalloy INCONEL MA 6000, which is also produced by the mechanical alloying process. Being a candidate material for advanced gas turbine blades operating at increased temperatures, this alloy has been studied extensively, especially in a recent European Cooperative Programme (COST 501). Grain boundaries are particularly detrimental in such a highly strengthened material; therefore this alloy is commonly recrystallized by zone annealing to obtain an extremely elongated, coarse grain structure, with typical grain size in the millimetre range and grain aspect ratios of 10 to 20 (Ref. 4). In this condition the alloy exhibits high stress sensitivity which can be interpreted in terms of a temperature-dependent 'threshold stress' (Fig. 4, from Ref. 4). This trend is also seen in compression testing at higher strain rates.[32] The extensive data base for stress rupture also reflects a high stress sensitivity which appears to increase with temperature and rupture time.[33] In the as-extruded fine-grain condition creep rates are many orders of magnitude faster;[30] in fact the alloy exhibits superplastic behaviour which allows forming of components by isothermal forging.[34]

(a)

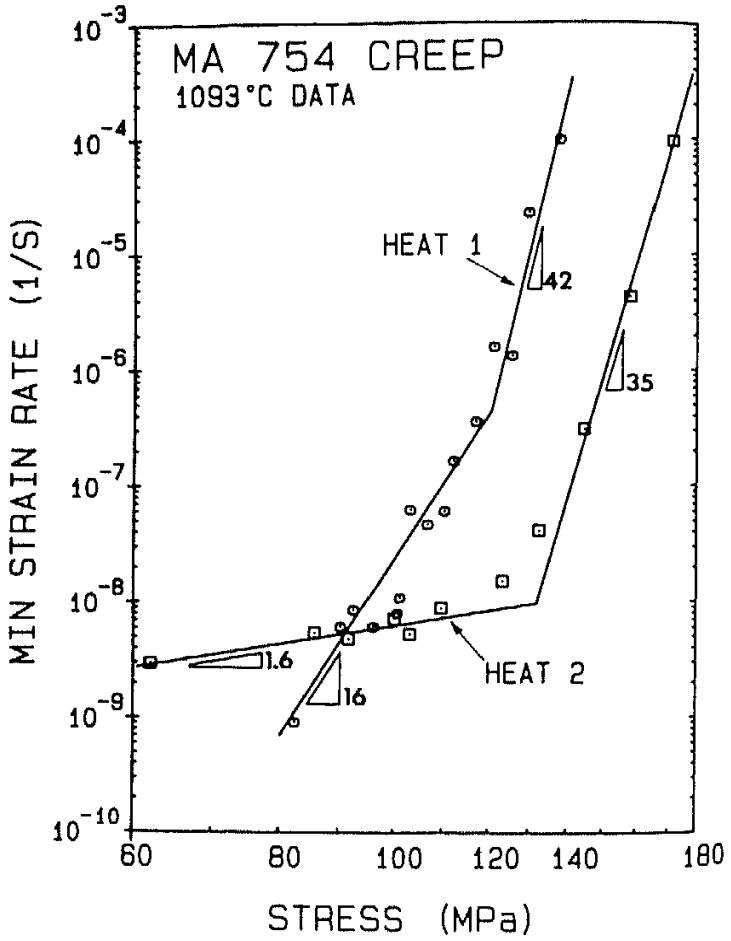

(b)

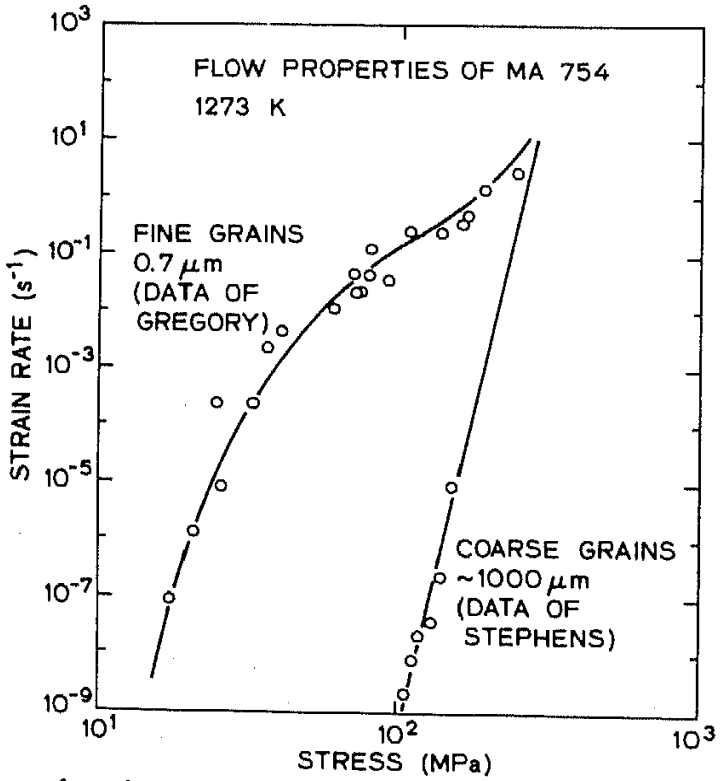

Fig. 3. The influence of grain morphology on the creep properties of the nickel base alloy Inconel MA 754: (a) comparison between material with a uniform elongated grain structure ('heat 1') and an elongated grain structure with fine-grain pockets ('heat 2') (from Refs 29 and 118); (b) comparison of coarse-grained (recrystallized) with fine-grained (as-extruded) material (Ref. 31, data from Refs 29 and 30).

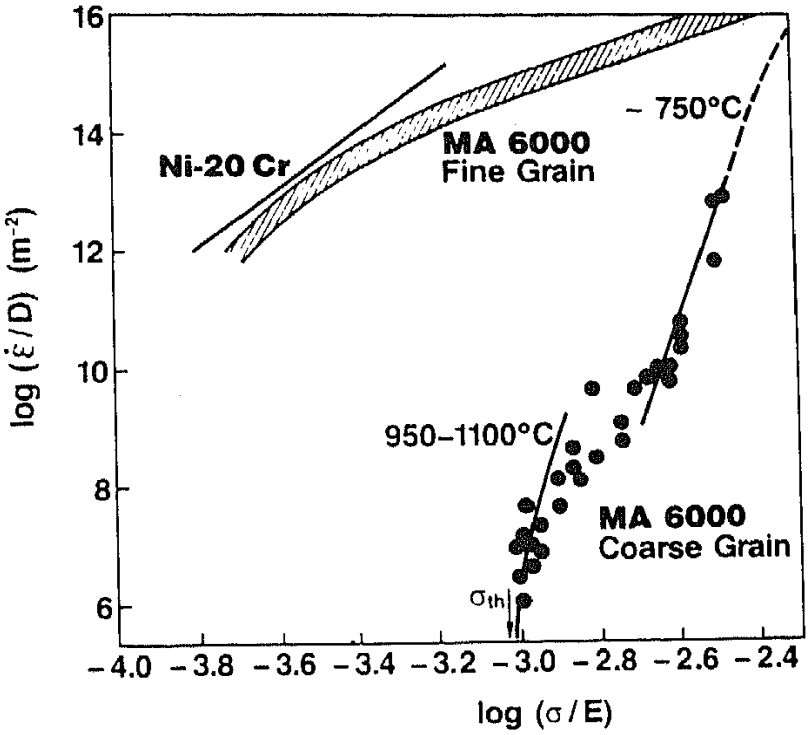

Fig. 4. 'Threshold stress' behaviour of coarse-grained alloy Inconel MA 6000, compared with fine-grained material and dispersoid-free Ni–20Cr. Note apparent temperature dependence of the 'threshold stress' (compare Fig. 14) (from Ref. 4).

Two important effects of grain structure on creep behaviour have been studied in this alloy: the influence of the grain morphology on rupture life[35,36] and the role of recrystallization defects as crack starters.[36] Although the grain dimensions could not be varied independently during zone annealing, it was concluded that the grain aspect ratio (GAR) is decisive for rupture strength. The effect is dramatic, leading to a reduction of creep life at low GAR by two orders of magnitude (Fig. 5); this deterioration is caused by a transition to intergranular failure due to the growth of creep cavities on transverse grain boundaries. Fine grains, which consitute recrystallizations defects and do not necessarily differ in chemical composition from the otherwise coarse-grained matrix, are particularly susceptible to the formation of creep damage. They reduce creep life by acting as starting points for transgranular cracks. The property degradation which results from this mechanism has been found to be even more aggravated under combined creep-fatigue loading.[37,38]

An important corollary of the severe vulnerability of grain boundaries in ODS materials is a pronounced anisotropy of tensile creep properties. While (short-term) tensile strength[39] and short-term compressive creep strength[32] are relatively insensitive to loading direction with respect to the extrusion axis (grain elongation), tensile creep

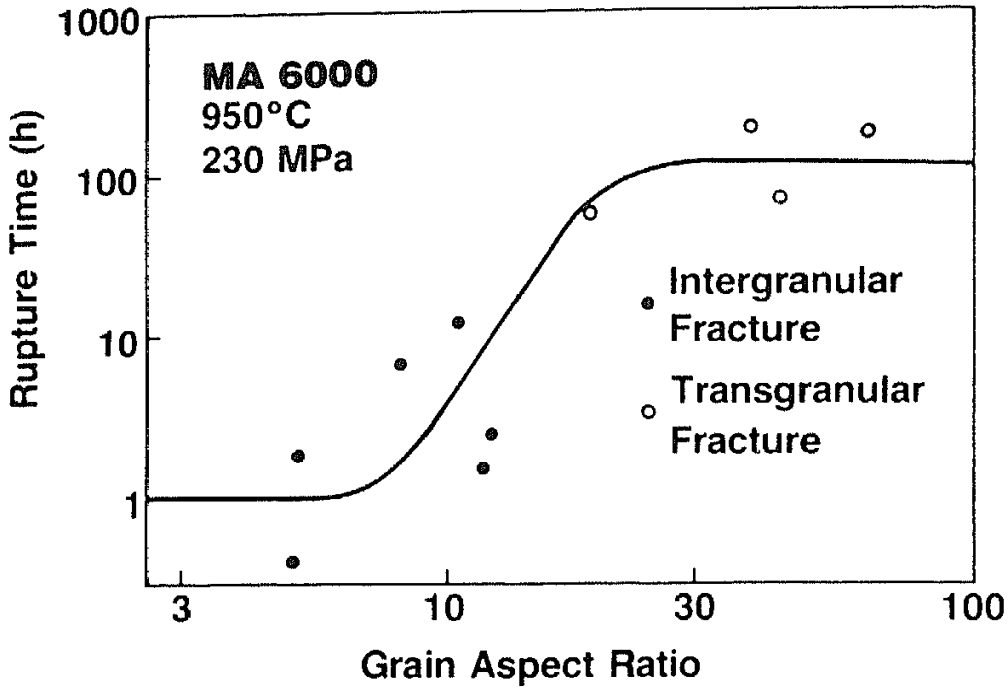

Fig. 5. Creep rupture time of coarse-grained Inconel MA 6000 as a function of grain aspect ratio after recrystallization by zone annealing (from Ref. 4).

strength is substantially reduced in the transverse directions[40] (Fig. 6(a)). The reason is again the occurrence of premature intergranular fracture at the longitudinal grain boundaries, with a concomitant severe reduction in ductility. At low stresses creep rates are affected even under compressive transverse loading, which leads to considerable deformation below the 'threshold stress'.[40] This type of loading produces γ'-free diffusion zones on grain boundaries parallel to the compression axis (Fig. 6(b)), which has been interpreted as being indicative of a contribution by diffusion creep. What is atypical of diffusion creep, however, is the high stress exponent that applies in this regime.

Similar evidence for diffusion creep has been found earlier by Whittenberger,[41] who points out that the depleted zones will be vulnerable to corrosion attack. The author identified substantial 'threshold stresses' (up to 90 MPa) in several dispersion strengthened materials with medium grain size and attributed them to an inhibition of diffusion creep due to the presence of the dispersoid particles (which is highly debatable—see also Section 4). These threshold stresses decreased strongly with increasing temperature and were apparently dependent on the grain structure: for several alloys they increased linearly with the grain aspect ratio, evaluated in the appropriate direction.[42] Apparent 'threshold stresses' for diffusional creep have also been reported in other fine-grained dispersion strengthened materials:

(a)

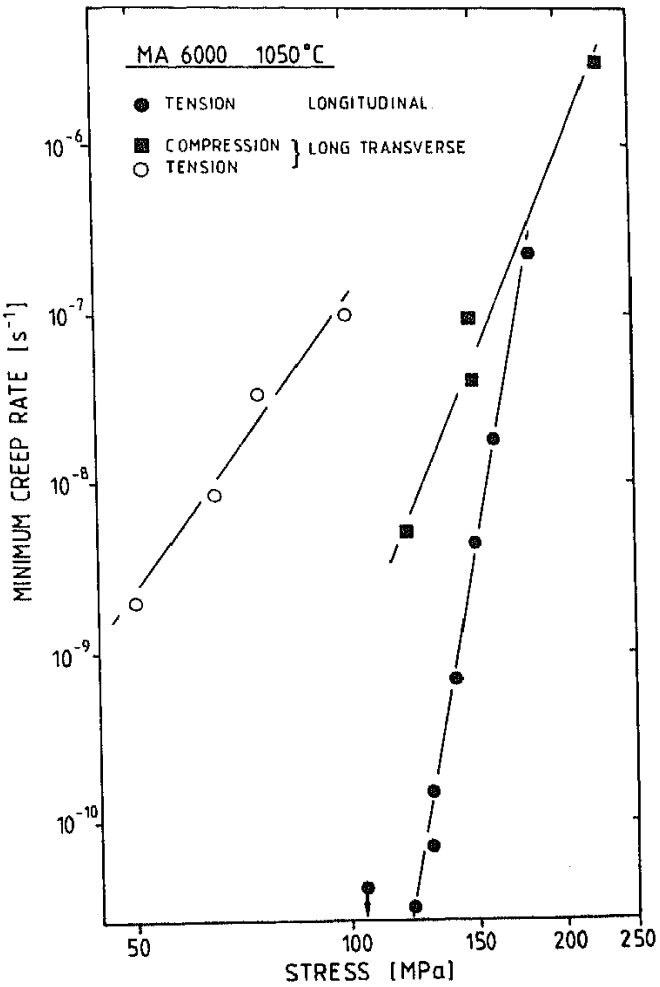

(b)

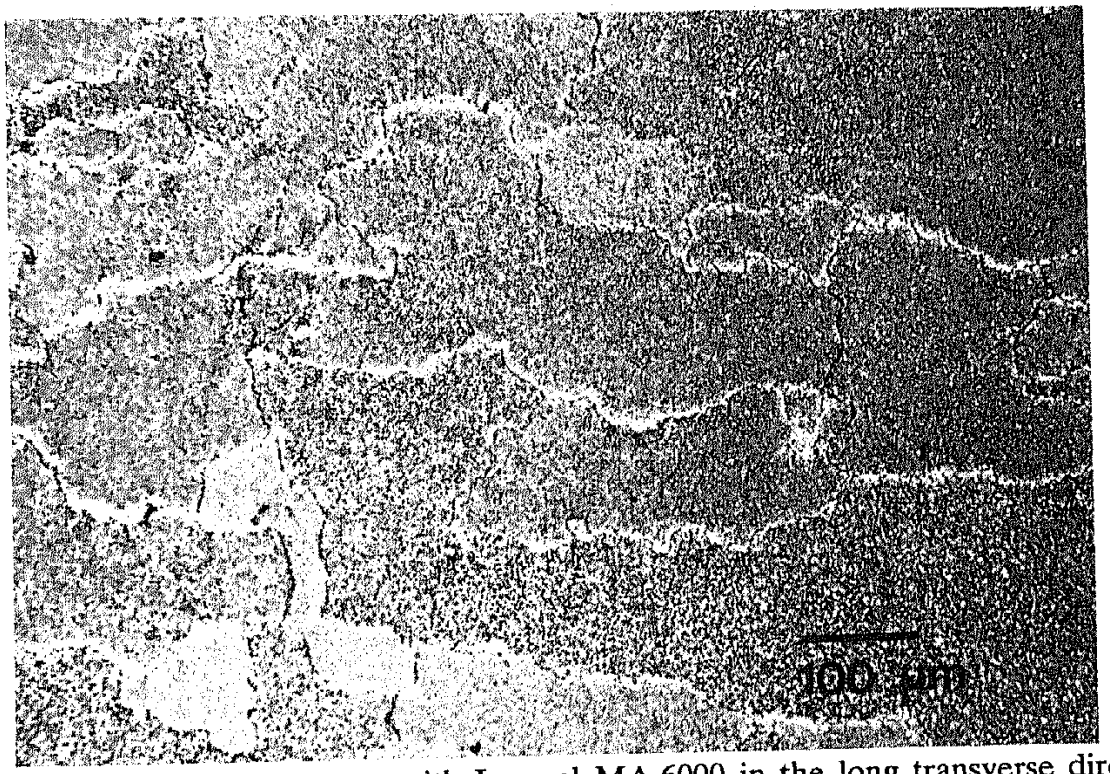

Fig. 6. Results of creep tests with Inconel MA 6000 in the long transverse direction (from Ref. 40): (a) comparsion of creep rates, under tension and compression, with longitudinal data (tension); (b) evidence for diffusion creep in the form of precipitate-free zones on a transverse section after compressive loading in the long transverse direction.

in $Au–Al_2O_3$,[43] $Cu–Al_2O_3$,[44,45] $Cu–SiO_2$,[46] in stainless steels with grain-boundary carbides[47–51] and in $NaCl–Al_2O_3$.[52] In all these cases, however, the measured 'threshold stresses' were only of an order of magnitude 1 MPa, which appears to be of little practical significance. Also, experimentation becomes delicate in this region, and the 'threshold stress' issue is somewhat controversial. Clegg and Martin[46] and Clegg[53] deny its existence, preferring an interpretation of the high stress sensitivity in terms of coupled processes which give rise to an 'apparent' threshold behaviour. No doubt, the evidence for 'threshold stress' behaviour is much less clear-cut in diffusion creep than in dislocation creep and will not be considered further.

2.1.2 *Aluminium alloys*

Early investigations with SAP in the 1950s generally lacked quantitative microstructural characterization of the dispersoids and were not systematic enough to allow definitive conclusions regarding creep mechanisms (e.g. Ref. 54). Extensive creep studies were performed on Al with up to 10 vol% Al_2O_3 by Milicka *et al.*;[55] see also Cadek.[56] Cadek identified 'threshold stresses' which amounted to about 42–62% of the Orowan stress as inferred from tensile test data and were not systematically dependent on volume fraction.

The creep behaviour of well-characterized SAP-type material (Al

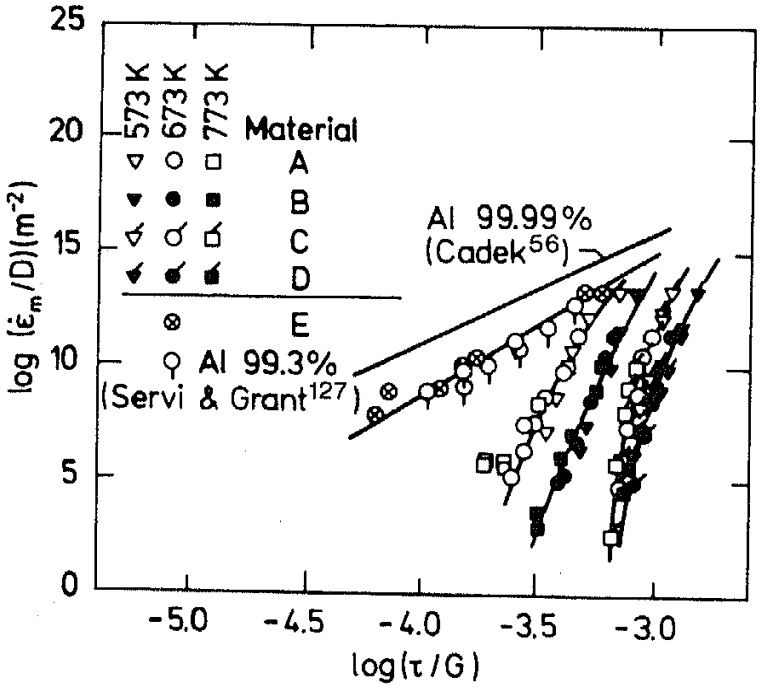

Fig. 7. Creep properties of four $Al–Al_2O_3$ materials with different volume fractions of dispersoid (A, B, C, D), compared with dispersoid-free aluminium (E, Al99·99% and Al99·3%). Data at 873 K deviate significantly and are not included (from Ref. 57).

with 0·19 to 0·92 vol% Al_2O_3 in the form of platelets) was studied and interpreted by Clauer and Hansen.[57] These alloys had been recrystallized to grain sizes in the millimetre range, with remarkably high GAR values of up to 40. The creep data, when compared with those of pure Al (Fig. 7), are again indicative of a 'threshold stress' behaviour. The interpretation of the data is complicated by the fact that the stress sensitivity is reduced at the higher testing temperatures, especially in the low-volume fraction alloy variants (data points not included in Fig. 7); this onset of weakening is attributed by the authors to grain boundary sliding.

Mechanically alloyed aluminium with carbide and oxide dispersoids was creep tested in the as-extruded, (presumably) fine-grained condition by Oliver and Nix,[58] and showed high stress exponents ($n \approx 25$) at $\sigma/E = 10^{-3}$. Adding Mg to the alloy (alloy IN 9051) resulted in an unexpected weakening effect (Fig. 8): not only were considerable creep rates detected at stresses below $10^{-3}E$, but the dispersion strengthened material was even inferior to a dispersion-free Al–Mg solid solution at higher stresses. The authors offered an explanation for these effects in terms of loss of solute clouds along dislocations which rapidly pinch off

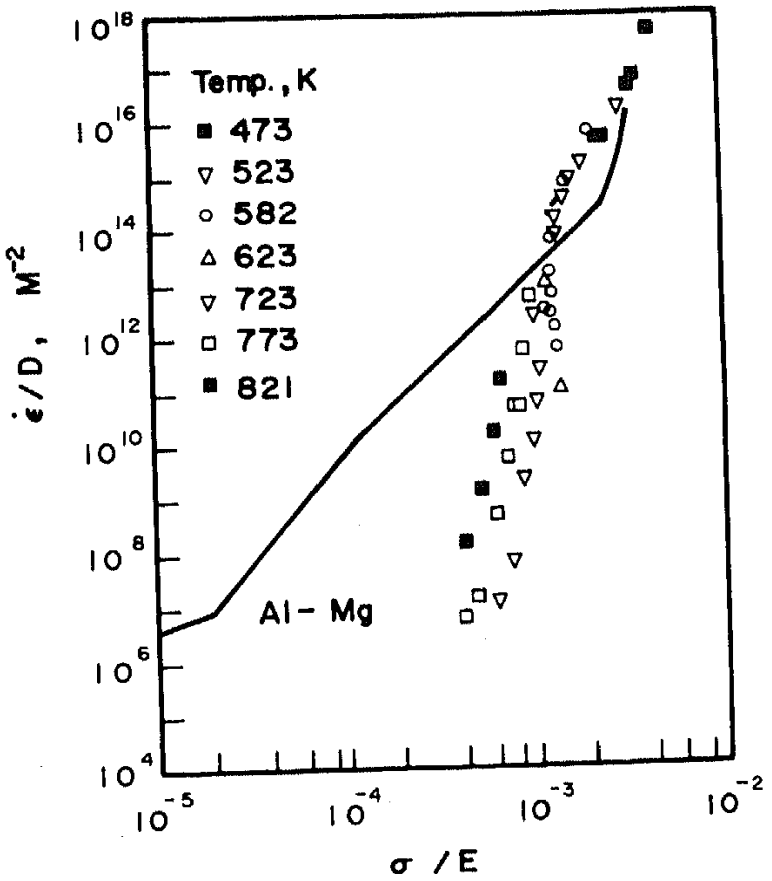

Fig. 8. Creep properties of dispersion strengthened Al–Mg at various temperatures (symbols), compared with dispersoid-free Al–Mg (line) (from Ref. 58).

behind the dispersoid particles and of the greater deformability of MgO, which is shown to replace the Al_2O_3 dispersoids in this variant.

Otsuka *et al.*[59] investigated the creep and creep fracture behaviour of a similar solid solution and dispersion strengthened alloy with fine grains (alloy IN 9052) after heat treatment. Extremely high n values ($n \approx 70$–150) were reported at intermediate stresses, with a lower stress sensitivity above and below (Fig. 9), but no clear interpretation of the resulting sigmoidal curves is given. Somewhat different results were found by Orlova *et al.*[60] for the same alloy without heat treatment. They report a high apparent activation energy for creep ($Q_c = 398$ kJ/mole) and only moderate stress exponents ($n = 12{\cdot}2 \pm 0{\cdot}4$). Ductility was found to increase sharply with increasing stress/strain rate.

A precipitation and dispersion strengthened fine-grained Al alloy (alloy IN 9021) was studied by Kucharova *et al.*[61] Pronounced secondary creep, with short primary and tertiary stages, was found at temperatures between 623 and 723 K, with extremely high activation energies ($Q_c = 712 \pm 40$ kJ/mole) and moderate stress exponents ($n = 16{\cdot}2 \pm$

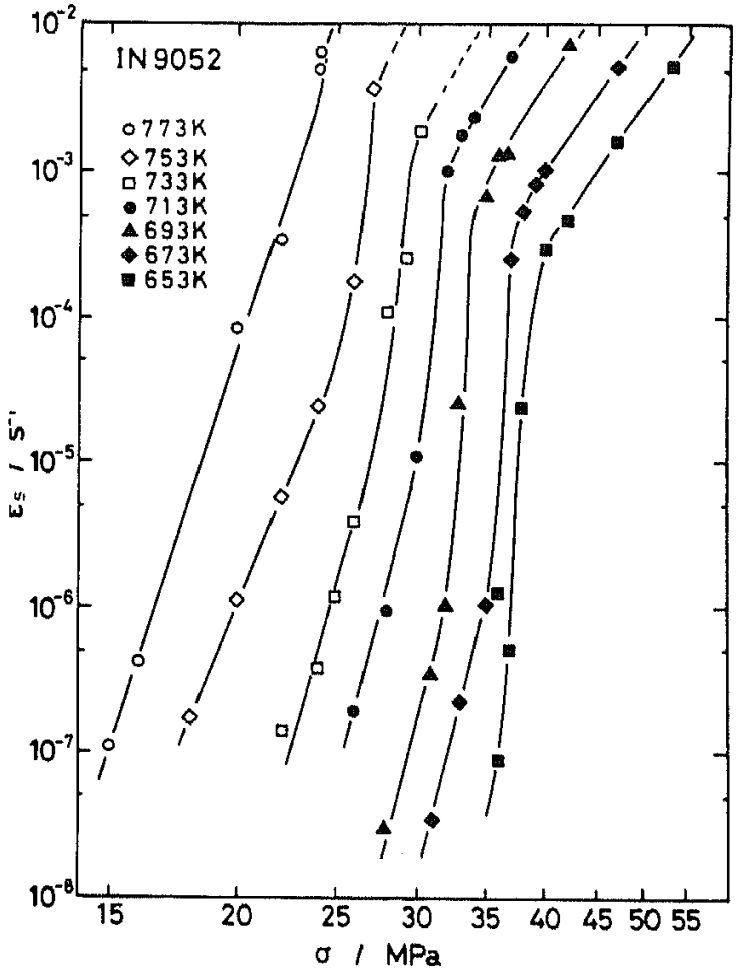

Fig. 9. Creep data for the dispersion strengthened aluminium alloy IN 9052, resulting in sigmoidal curves (from Ref. 59).

1·2). A slightly sigmoidal shape is apparent in the creep data. In view of the small grain size, the authors favour an explanation of their observations in terms of interface-controlled diffusion creep,[62] but admit that the evidence is not clear-cut and that several inconsistencies remain. Superplasticity has been reported in this alloy at relatively high strain rates by Nieh *et al.*[63]

The creep behaviour and dislocation structures of Al and Al–Si containing Al_2O_3 dispersoids were studied in the temperature range 473–873 K by Matsuda and Matsuura.[64] While typical 'threshold stress' behaviour was found below 673 K, a strong weakening effect was reported at higher temperatures and low stresses, especially for a fine-grained variant. Estimation of the relative contribution of grain boundary sliding to overall strain, by means of marker line observation, gave only about 10–30%. The loss of 'threshold behaviour' is attributed qualitatively to a coupling between grain boundary sliding and grain deformation. TEM revealed considerable dislocation densities, with well-defined sub-boundaries occurring only at temperatures in excess of 773 K. The fracture behaviour depended characteristically on the strain rate: at high creep rates ($\dot{\varepsilon}/D$), elongations were large (~10%), necking occurred and the fracture surfaces showed deep ductile dimples; at low $\dot{\varepsilon}/D$, many flat regions with shallow dimples were observed, necking was scarcely detectable, and fracture strains were small—typical characteristics of intergranular fracture.

The compressive and tensile creep strength and the microstructure of reaction-milled Al and Al–Mg alloys have been studied extensively by Arzt and Rösler,[65] Rösler[66] and Joos[67] (for selected results see Fig. 10). Even the fine-grained alloys exhibit a region of extremely high stress sensitivity ($n > 50$), which tends to decrease at high temperatures and low strain rates (low $\dot{\varepsilon}/D$) suggesting again a sigmoidal shape. The fact that the data for different temperatures do not coincide on the temperature-compensated plots (Fig. 10) indicates that the activation energy is higher than that for volume diffusion: an Arrhenius plot yields values up to 537 kJ/mole, compared to 142 kJ/mole for volume diffusion in aluminium.

In order to test the hypothesis that the weakening effect at low $\dot{\varepsilon}/D$ was due to grain boundary effects, the Al–Al_2O_3 variant (AlCO) was also compression tested in a recrystallized state with typical grain dimensions $3 \times 0{\cdot}2$ mm, corresponding to a grain aspect ratio of about 15. The stress sensitivity then remains high ($n > 80$) down to low strain rates and creep strength up to 30% higher than in the fine-grain condition is achieved. This improvement is even more pronounced in tension (Fig. 11) where, however, the deformation behaviour is

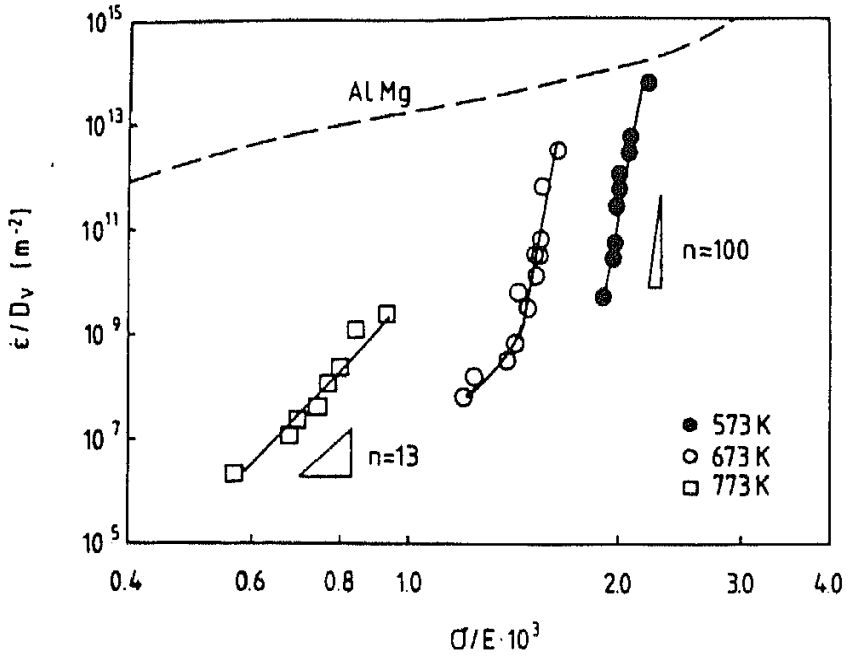

Fig. 10. Creep properties of dispersion strengthened Al–4Mg at various temperatures. Despite normalized axes, the data do not fall on a single curve; 'threshold stress' behaviour is lost at low $\dot{\varepsilon}/D_V$ (from Ref. 65).

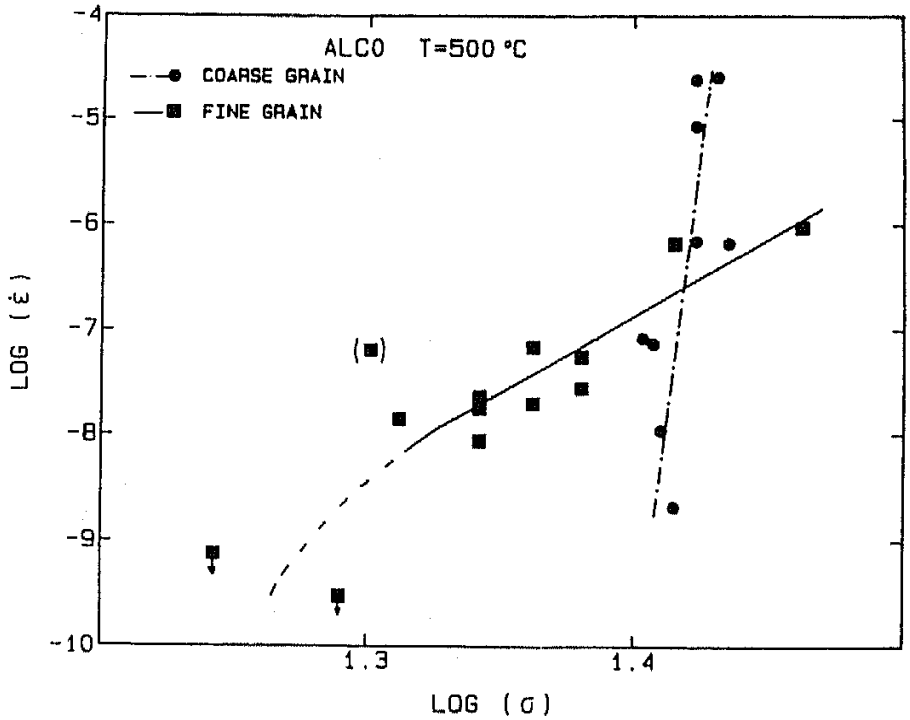

Fig. 11. Comparison between creep properties of fine- and coarse-grained Al–Al_2O_3 (from Ref. 67).

strongly influenced by material defects in the form of underprocessed powder particles.[68] These defects are also responsible for the lower creep ductility of the coarse-grained material; this is in contrast to TD–NiCr which is more ductile as a single crystal than in the fine-grained condition.[25] Finally, accidental recrystallization of fine-grained alloy AlCO to a fine grain size resulted in a substantial weakening by about 30% instead of an improvement in creep strength. This effect, which obviously would have to be avoided during alloy processing, was interpreted by Joos[67] to be due to the development of an unfavourable new texture by primary recrystallization.

Similar Al–Al_4C_3 alloys were investigated by Slesar *et al.*[69] with regard to high-temperature flow strength and ductility. A tension/compression asymmetry of the (0·2% offset) flow stress was noted, which increased with rising temperature to about 50% and was almost independent of carbide volume fraction. In view of the dimpled structure of the fracture surfaces, the authors ascribe this effect to the debonding of larger carbide dispersoids from the matrix under tensile load (in analogy to the results of Olsen and Ansell[70] for TD–Ni). The fall in elongation with increasing temperature is explained by an enhanced susceptibility to debonding at higher temperatures. However, grain boundary processes cannot be totally excluded as being responsible for such ductility and asymmetry effects.

Recently, attempts have been made to combine the high temperature advantages of dispersion strengthening with the higher stiffness which can be obtained in rapidly solidified materials containing intermetallic precipitates. By a mechanical alloying technique, Yaney *et al.*[71] introduced carbide and oxide dispersoids in Al–Fe–Ce powder produced by rapid solidification and compared the compressive creep properties of the resulting material (MA–Al–Fe–Ce) with the non-MA counterpart (Fig. 12). At 523 K, both alloys have nearly equal strength and are considerably stronger than mechanically alloyed Al tested by Oliver and Nix.[58] All three alloys clearly exhibit high stress exponents ($n \approx 30$). As the temperature is increased to 773 K, the strength of Al–Fe–Ce decreases sharply and also the stress sensitivity falls considerably ($n \approx 6$). By contrast, the MA–Al–Fe–Ce retains its high strength and stress sensitivity at this temperature; interestingly, the activation energy for creep ($Q_c = 157$ kJ/mole) corresponds closely to that for volume diffusion in aluminium. At a strain rate of 10^{-5} s^{-1} MA–Al–Fe–Ce is six times stronger than Al–Fe–Ce and still significantly stronger than MA–Al.

The authors show by annealing and retesting that the strength reduction in Al–Fe–Ce cannot be due mainly to recovery processes or

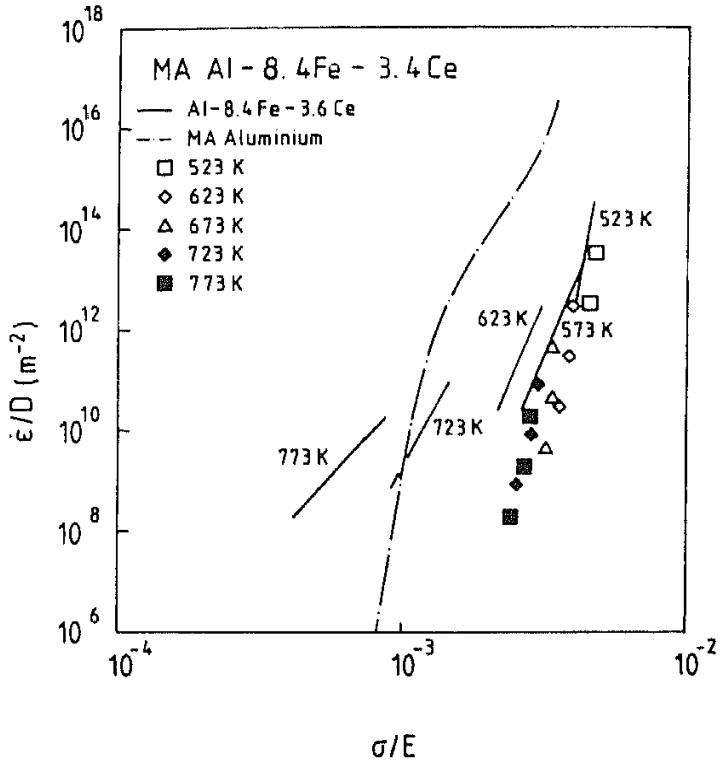

Fig. 12. Creep data of a rapidly solidified Al–Fe–Ce alloy containing also oxide and carbide dispersoids (symbols), compared with dispersoid-free Al–Fe–Ce (lines) and dispersion strengthened aluminium (dash-dotted line) (from Ref. 71).

particle coarsening; instead a reversible loss in particle strength at high temperatures is made responsible for this weakening effect, which does not occur with the stronger oxide and carbide dispersoids in the MA variant. This speculation on particle strength is consistent with the concept of dispersoid efficiency (to be discussed in Section 3.1), which will be shown to offer a quantitative explanation for the strength differences observed here. Grain size is concluded to have only a minor effect, although the mechanically alloyed powder apparently recrystallized during subsequent extrusion from about 1 μm to a grain size of 30 μm. We note in passing that the weakening effect of the non-MA variant seen in Fig. 12 is typical of rapidly solidified aluminium alloys and occurs also, for example, in advanced Al–Fe–V–Si materials.[72]

2.1.3 *Other alloy systems*

The dispersion strengthened ferritic alloy Incoloy MA 956, which is produced by mechanical alloying, also exhibits a high stress exponent when creep-tested in a coarse-grain or single-crystal condition.[73] By contrast, creep of the fine-grain variant is only weakly stress-dependent and does not show 'threshold stress' behaviour. Finely dispersed carbide particles, too, can act as efficient dispersoids in ferritic steels;

Peterseim and Sauthoff[74,75] found 'threshold stresses' which varied characteristically with carbide volume fraction.

A special class of dispersion strengthened high temperature materials is tungsten wires with a dispersion of potassium bubbles ('K-doped tungsten'). The creep behaviour of such wires with grain aspect ratios between 10 and 60 has been studied in the temperature range 2400–3100 K by Pugh[76] and Wright.[77] At high GAR, the stress exponent is $n \approx 25$ and the apparent activation energy exceeds that for volume diffusion (620 kJ/mole) by a factor of 2·5 (1600 kJ/mole). Low-GAR material exhibits low stress sensitivity ($n \approx 5$) and intergranular creep fracture—this behaviour is completely analogous to that of Inconel MA 6000. While doping with potassium also stabilizes a high GAR, the grain elongation effect is not sufficient to explain the improvement of creep strength in this alloy. The 'dispersoids', which are K-vapour filled pores at creep temperatures, have been shown to be strong obstacles to dislocation motion. This example illustrates that pores, though shearable, can be efficient 'dispersoids' up to very high absolute temperatures. The filaments, for which these wires are used, are probably among the applications of metallic materials at the highest homologous temperatures to date ($T \approx 0{\cdot}8T_M$).

2.2 Summary of phenomenological results

1. It is well established that dispersoid particles cause a pronounced retardation of creep. In general the steady-state creep behaviour of dispersion strengthened materials at a given temperature gives rise to sigmoidal log $\dot{\varepsilon}$–log σ curves with three more or less distinct regions (Fig. 13): at high strain rates the material approximates the behaviour of the dispersoid-free counterpart, with 'normal' stress exponents and activation energies (region I); at intermediate strain rates there exists usually a region of 'anomalously' high stress sensitivity ($n \cong 20$–100) and high apparent activation energy (region II); finally at high temperatures and low strain rates the stress exponent may decrease again (region III).
2. Region II, which can extend over up to eight orders of magnitude in strain rate, is generally more pronounced in coarse-grained and single crystal materials; other, mostly fine-grained, dispersion strengthened alloys show only moderate stress sensitivities ($n \approx 10$) which are still considerably higher than in the dispersion-free materials. In at least three instances—fine-grained MA 754, MA 6000 and IN 9021—indications for

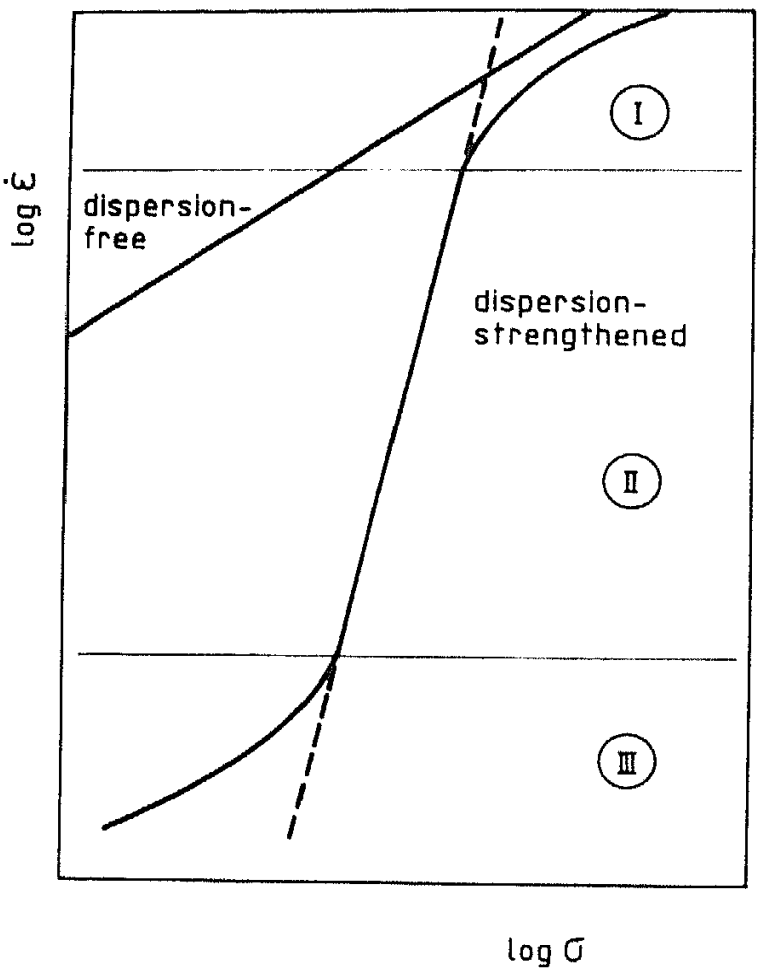

Fig. 13. Schematic of the creep rate as a function of stress in dispersion strengthened and dispersion-free materials. The curvature in 'region III' has been reported usually only for very high temperatures.

superplasticity with low n values have been reported. Obviously, a 'universal' stress exponent for creep in dispersion strengthened materials does not exist.

3. The reduced stress sensitivity in 'region III' in Fig. 13 amounts to a loss of strength (compared to extrapolations from region II). It has been reported for polycrystals as well as single crystals at very high temperatures and low strain rates. Ad-hoc explanations involve dissolution, coarsening or deformation of dispersoid particles and/or onset of grain boundary processes. This 'region III' behaviour has been less well characterized than 'region II' but may become important under service conditions.
4. The temperature dependence of the creep rate is often observed to be 'abnormal' in the sense that temperature-compensated plots of log $\dot{\varepsilon}/D_V$ versus log σ/E do not produce a single curve for different temperatures (e.g. Figs 8 and 10). This implies that the apparent activation energy for creep is higher than that for

volume diffusion. In other cases the creep data can be normalized successfully in this way (e.g. Fig. 2(b)).

5. The role of grain boundaries in creep of dispersion strengthened materials is not clear-cut. In highly strengthened mechanically alloyed Ni and Fe base alloys grain boundaries are favoured sites of creep damage initiation, which is minimized in coarse grains with high aspect ratios. The detrimental role of grain boundaries in these alloys is also reflected in the poor transverse tensile creep properties. By contrast, most dispersion strengthened Al alloys, which generally contain higher volume fractions of dispersoids, exhibit high creep strength (at similar homologous temperatures) even with submicron grains, and apparently do not fracture along grain boundaries. When subjected to low stresses, fine-grained alloys sometimes show evidence for deformation by diffusion creep which also appears to be subject to a 'threshold-like' behaviour; the evidence, however, is not so clear and is probably of little practical significance.
6. Dispersoids generally lower the ductility. In the few instances where information on creep ductility is available, it increases strongly with increasing strain rate/creep stress (for both fine-grained Al and single-crystal TD–NiCr). Tensile deformation is often reported to be highly inhomogeneous. A tension/compression asymmetry of the flow stress has been reported for Al–Al_4C_3. Dispersoid–matrix decohesion, plastic instability and/or grain boundary damage may play a role for asymmetry and ductility effects.

2.3 Formal rationalization of a high stress sensitivity: 'threshold stress' concept

The high stress sensitivity in region II has captured most attention in the literature. Its existence is inconsistent with the general description of dislocation creep in terms of a semi-empirical power-law function of the applied stress (e.g. Ref. 78):

$$\dot{\varepsilon} = A \frac{D_V G b}{k_B T} \left(\frac{\sigma}{G}\right)^n \tag{1}$$

where $\dot{\varepsilon}$ is the strain rate, σ the applied stress, D_V the volume diffusivity, G the shear modulus, b the Burgers vector, k_B Boltzmann's constant, T the absolute temperature, A a dimensionless constant, and n the stress exponent. While for dispersoid-free materials n is generally found to lie between 3 and 10, dispersion strengthened materials exhibit

'anomalously' high n values which cannot be explained on the basis of current theories of power-law creep.

The temperature dependence of the creep rate can be characterized by determining an 'apparent' activation energy for creep:

$$Q_{app} = -R\left[\frac{d(\ln \dot{\varepsilon})}{d(1/T)}\right]_{\sigma=const} \tag{2}$$

This value has to be corrected for the temperature dependence of the modulus[79] in order to obtain a corrected activation energy for creep in eqn (1):

$$Q_C = Q_{app} + RT - (n-1)\frac{RT^2}{G}\left(-\frac{dG}{dT}\right) \tag{3}$$

This correction serves to lower the activation energy (e.g. Refs 25 and 80), but in most cases the resulting value is still considerably in excess of the activation energy for volume diffusion.

Because of these shortcomings of eqn (1), a modified constitutive equation containing a 'threshold stress' σ_0 has been proposed for dispersion strengthened materials:[81,82,9]

$$\dot{\varepsilon} = A'\frac{D_V G b}{k_B T}\left(\frac{\sigma-\sigma_0}{G}\right)^{n'} \tag{4}$$

This expression gives an arbitrarily high 'apparent' stress exponent at stresses just above σ_0:

$$n_{app} = \frac{d(\ln \dot{\varepsilon})}{d(\ln \sigma)} = \frac{n\sigma}{\sigma-\sigma_0}\left(1-\frac{d\sigma_0}{d\sigma}\right) \tag{5}$$

(Note that this equation reduces to $n_{app} = n$ if $\sigma_0 = 0$ or $\sigma_0 \propto \sigma$.) By allowing σ_0 to decrease with increasing temperature, a still higher 'apparent' activation energy can in principle be formally justified:

$$Q_{app} = Q_V - RT + \frac{RT^2}{G}\left(-\frac{dG}{dT}\right)(n-1) + \frac{nRT^2}{\sigma-\sigma_0}\left(-\frac{d\sigma_0}{dT}\right) \tag{6}$$

The additional correction term in eqn (6) becomes significant at stresses close to σ_0 and at high n. It should be mentioned that some authors (e.g. Ref. 56) claim that their data, especially at the high stress end, cannot be described by an expression of the form of eqn (4) but conform to an exponential or sinh-relationship ('power-law breakdown'). A 'threshold stress' σ_0 usually also appears in these expressions.

It must be emphasized that the 'threshold stress' σ_0 cannot be a true threshold for creep deformation, in the sense that at stresses below it

the strain rate is identical to zero—as is suggested by the form of eqn (4). With further mechanistic background, this modified constitutive equation will be seen merely as an approximation which permits a more consistent description of creep data in the range measured experimentally. Consequently, there is no physical justification whatsoever for using eqn (4) when extrapolating into temperature–stress ranges which have not been experimentally investigated, especially towards low $\dot{\varepsilon}/D_V$. In fact, it will be shown in Section 3 that recent models for the mechanism of dispersion strengthening at high temperatures lead to serious conceptual reservations concerning uncritical use of a 'threshold stress' concept.

Bearing these qualifications in mind, one can still attribute some practical significance to the value of the apparent 'threshold stress' σ_0 as it characterizes the stress level at which dispersion strengthened materials become far superior to their dispersoid-free counterparts. Further, for practical applications the 'threshold stress' will be a design-limiting strength property: service stresses must always be kept below it in order to avoid occurrence of undesirable creep deformation.

Threshold stress values have been determined by various authors for several dispersion strengthened alloy systems, including thoriated NiCr, Al–Al_2O_3, and the mechanically alloyed iron-base alloys MA 956, MA 754 and MA 6000. Unfortunately, it is not always possible to compare these thresholds because they have been extracted from the creep data in different ways. One possibility is to estimate a 'threshold stress' from the curved log $\dot{\varepsilon}$–log σ plot by assuming that the creep strength of the matrix and that due to the dispersoids superimpose linearly.[25,27] Another way is to replot the data in linearized form, as $\dot{\varepsilon}^{1/n}$ versus σ, which according to eqn (4) allows linear extrapolation to zero strain rate (e.g. Refs 32, 83 and 75). In the latter approach, the choice of n is critical and there is no agreement between various authors on which n to choose. Some authors prefer to force-fit the data to theoretical values $n = 3{\cdot}5$ (Ref. 32) or $n = 4$ (Ref. 61). In the latter study 'back stresses' are evaluated which are not true threshold stresses; they vary characteristically with the applied stress in a way which reproduces the sigmoidal shape of the log $\dot{\varepsilon}$–log σ plot.

For the sake of comparison, an attempt will be made here to evaluate 'threshold stresses' from published creep data in a consistent way. In order to preclude grain boundary effects, only data from 'region II' for single crystals or coarse elongated grains (tested in the longitudinal direction) are included. The data were plotted as $(\dot{\varepsilon}/D_V)^{1/n}$ versus σ/E (where E is Young's modulus) and extrapolated linearly to $\dot{\varepsilon} = 0$. The diffusivity normalization produced in most cases parallel lines for

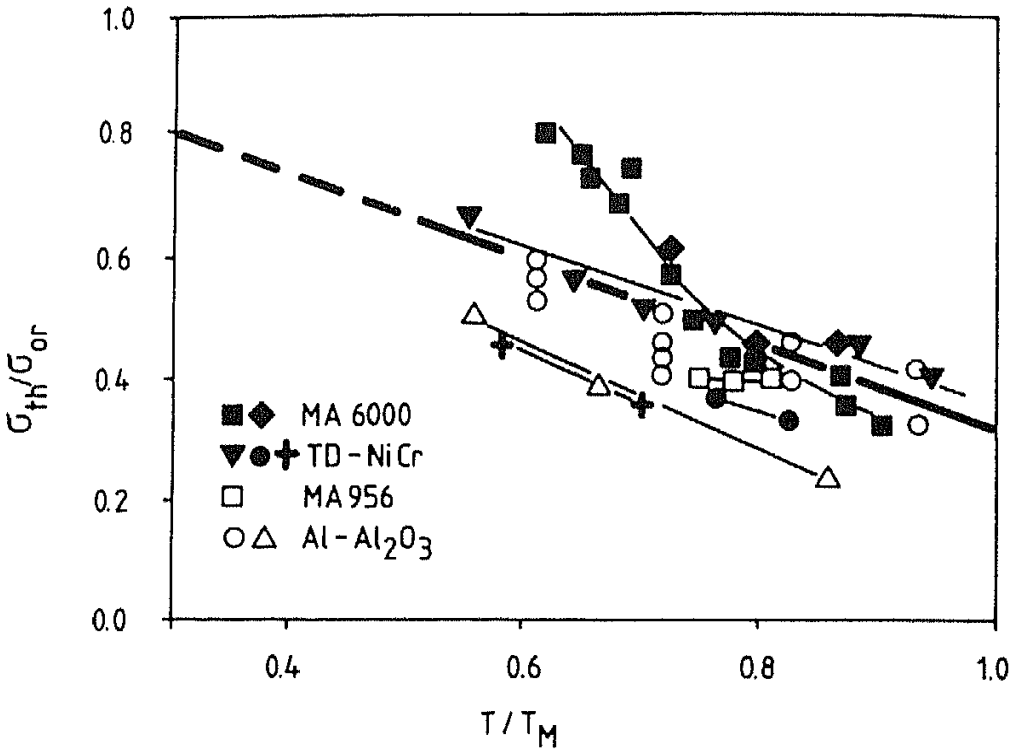

Fig. 14. Plot of experimental 'threshold stresses', normalized with respect to the calculated Orowan stress, as a function of homologous temperature, for coarse-grained or single crystal materials: MA 6000 (Refs 32, 33), TD–NiCr (Refs 25, 16, 95), MA 956 (Ref. 73), Al–Al_2O_3 (Refs 57, 58).

different temperatures, which generally improved the reliability of the extrapolations. Rather than force-fitting the data to stress exponents suggested by theoretical considerations, values typical of the dispersoid-free material were chosen: for example $n = 4{\cdot}6$ for Ni–20Cr based ODS alloys.

The results are plotted in a normalized form in Fig. 14. Absolute temperatures have been divided by the melting point (or the approximate solidus temperature). The threshold stresses have been normalized with respect to the Orowan stress given by

$$\sigma_{Or} = \frac{0{\cdot}84\,M}{2\pi(1-\nu)^{1/2}} \frac{Gb}{l} \ln\left(\frac{r}{b}\right) \tag{7}$$

where M is the Taylor factor (or reciprocal Schmid factor for single crystals), ν is the Poisson number ($\nu = 0{\cdot}3$), l the mean planar particle spacing, and r the mean particle radius. In evaluating eqn (7), considerable error can be introduced because particle spacings and Taylor (or Schmid) factors are not always well known. The values for l were taken as quoted by the respective authors and M was calculated for the texture or single crystal orientation in question; for untextured polycrystals $M = 3$ was chosen. The justification for normalizing with

respect to σ_{Or} is that the theoretical threshold stresses all scale with σ_{Or} (see Section 3).

Despite the numerical uncertainties the following observations can be made in Fig. 14:

(1) The Orowan stress is a useful normalization parameter for 'threshold stresses', as it brings the data from very different materials, whose absolute threshold stresses differ by more than an order of magnitude, to within a factor of about 2. It appears plausible that similar mechanisms are responsible for the creep strength in these alloys.

(2) All the threshold stresses are below the theoretical Orowan stress, and decrease with increasing temperature. These deviations from the Orowan stress are important and will need to be explained theoretically.

In summmary, the 'threshold stress' concept appears to have some merit for formal rationalization of the creep behaviour in dispersion strengthened alloys. Without further mechanistic background, the applicability of this concept must, however, remain suspect. We therefore turn to the relevant theories of dispersion strengthening at high temperatures, which will be discussed in detail in the following section.

3 MECHANISMS OF CREEP STRENGTH IN DISPERSION STRENGTHENED MATERIALS

This section is entirely devoted to theoretical attempts to explain, in terms of dislocation theory, the high stress sensitivity of the creep rate ('threshold stress' behaviour) in materials with low volume fractions of dispersoids. The problem has received great attention over the past 15 years. Early papers attempted an explanation in terms of the Orowan process and its thermal activation.[84] But once the threshold stresses were found to be significantly lower than the Orowan stress of the particle dispersion, subsequent models focused on the process by which dislocations can circumvent hard particles, especially by climbing around them. Following detailed transmission electron microscopy of this process, more attention has been paid recently to the interaction between dispersoid particles and dislocations. New models have been proposed which abandon the idea of climb being the rate-limiting event. This development, including the latest results, is described below.

3.1 Dislocation climb models

When dispersoid particles are considered as impenetrable obstacles which force gliding dislocations to climb a certain distance until they can continue to glide, a retardation of creep is predicted, but a high stress sensitivity cannot be explained in this way; this has been realized early in the development of theories.[7,8,85] The maximum stress exponent which is obtained theoretically in this way is below $n = 4$.[86]

Only by realizing that the dislocation has to increase its line length in order to surmount the dispersoid can a climb-related 'threshold stress' be justified. This process has been modelled by Brown and Ham[87] and Shewfelt and Brown,[88] who assumed that climb is 'local'; this means that only the portion of the dislocation which is in close proximity with the particle–matrix interface undergoes climb while the remaining segment stays in the glide plane (Fig. 15(a)).

The infinitesimal change dU in internal energy when a climbing dislocation advances by dx is given by[14]

$$dU = d[\Gamma . L] - \tau bl\, dx - \sigma_n bl_c\, dz - dU_{el} \tag{8}$$

The first terms describes the change in elastic energy of the dislocation, either by a change in length L or by modification in specific line energy Γ. The second term is the work done by the applied shear stress τ during glide, while the work performed by the normal stress σ_n during climb of an 'active' segment of length l_c is represented by the third term. Finally the fourth term signifies the self-interaction of the bowed-out dislocation segments. Except for the models by Evans and Knowles[89] who (incorrectly) include only the normal stress contribution, and by McLean[90] who treats high volume fractions not considered here, the third term is usually neglected; this is reasonable for low volume fractions except for cases of special particle shape with $dx = 0$. The self-interaction term, which is important for calculation of the Orowan limit ('dipole interaction'), can also be disregarded to a first-order approximation; the typical breaking angles of dislocations under climb conditions can be shown to be far from the angle at which dipole interactions become relevant.[91]

For climb over the dispersoid to occur, internal energy must be gained everywhere along the dislocation path ($dU \leq 0$), which requires the stress to exceed a 'threshold stress' for local climb:

$$\sigma \geq \sigma_{th} = \frac{1}{2}\left(\frac{dL}{dx}\right)_{max} \frac{2\Gamma}{bl} \approx \frac{1}{2}\left(\frac{dL}{dx}\right)_{max} \sigma_{Or} \tag{9}$$

This threshold stress is proportional to the Orowan stress. The other

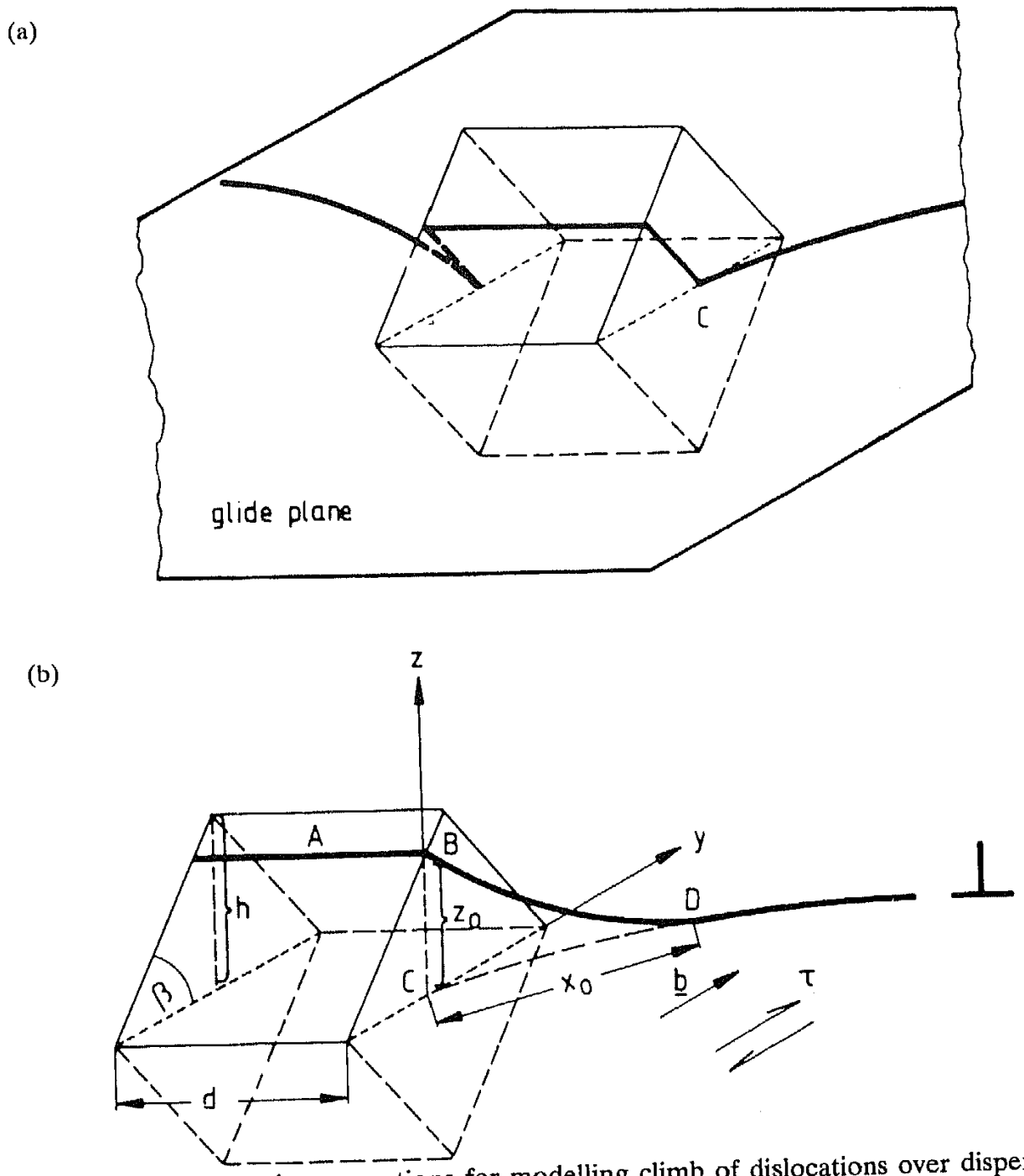

Fig. 15. Geometric assumptions for modelling climb of dislocations over dispersoids: (a) 'local climb' (Ref. 87); (b) 'equilibrium climb' (Ref. 96).

important parameter is the differential of the dislocation line length L with respect to advance distance x, at the point of its maximum. This quantity is called 'climb resistance'. During 'local climb' the dislocation profiles the particle contour and therefore the climb resistance is related to particle shape. A detailed analysis shows that the threshold stress amounts to about 70% of the Orowan stress for cubes oriented as in Fig. 15(a),[87] and to about 40% for spheres.[88]

The latter result was obtained by a computer simulation of local

climb in an array of hard particles intersected at random by the glide plane and therefore represents a statistical average. Arzt and Ashby[92] subsequently arrived at a similar result using a simple analytical model. We note that these threshold considerations lead to values which appear to be in the same range as experimental values (*cf.* Fig. 14). The temperature dependence, however, remains unexplained.

The kinetics of climb are solved by calculating the diffusion flux of vacancies arriving either (i) by core diffusion from the neighbouring particle (where the dislocation is assumed to be climbing in the opposite direction), or (ii) by bulk diffusion from the surrounding matrix (which is assumed to extend to infinity). Bulk diffusion, which dominates for $D_V > b^2 D_p/(2\pi rl)$, is generally thought to be rate-controlling.[11] The computer simulation of this case leads to the following constitutive equation, which does not contain any adjustable parameters:[10]

$$\log \frac{\dot{\varepsilon}}{D_V} = \log \left(\frac{8\pi^2 \tau_{Or} \tau^2 b}{2{\cdot}4 f_V k_B T G^2} \right) + \frac{1}{2{\cdot}3} \left[(15 \pm 3) \frac{\tau}{\tau_{Or}} - (10 \pm 1) \right] \qquad (10)$$

where f_V is the volume fraction of dispersoids.

It is interesting that this expression predicts an exponential dependence of creep rate on applied stress, although the bypass time for an individual particle varies only inversely with stress. The reason for this high stress dependence lies in the random distribution of dispersoids: each dispersoid which can be overcome by climb allows a number of its neighbours to be bypassed by the Orowan mechanism, and this number increases rapidly with stress. An exponential stress dependence of the individual bypass time would be predicted by the model of Humphreys *et al.*,[93] who consider jog nucleation to be the mechanism controlling dislocation climb (see also Martin,[17] p. 163). Contrary to Brown's approach, however, this model has not gained widespread acceptance.

While an equation of the form of eqn (10) may be applicable close to the threshold stress, it cannot reproduce the convex curvature of the creep plot as the creep behaviour approaches that of the dispersoid-free material (e.g. Fig. 2(b)). Therefore a semi-empirical equation has been proposed subsequently by Brown,[11] which is equivalent to a threshold-stress equation (eqn (4)) with $\sigma_0 = (3/8)\sigma_{Or}$ and $n' = 4$. Brown[11] has compared the data of Lund and Nix[25] on TD–NiCr and of Shewfelt and Brown[88] on Cu–SiO_2 with this equation (Fig. 16). Thus, while such a simple threshold-stress expression gives an 'adequate semi-empirical constitutive equation', its inadequacies are also quite clear. In particular, it cannot explain an approximately constant, high stress exponent or a remaining temperature dependence even when normalized vari-

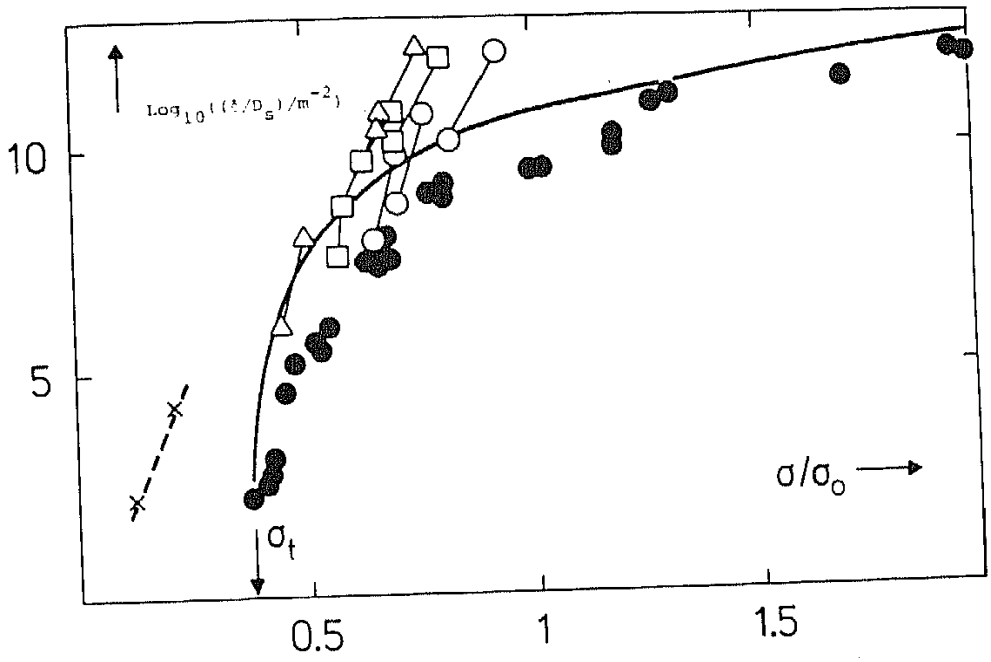

Fig. 16. Comparison between a 'threshold stress' creep law based on local climb and experimental data for TD–NiCr (solid circles, Ref. 25) and Cu–SiO_2 (open symbols, Ref. 88) (from Ref. 11).

ables are plotted, as evidenced by the data for TD–NiCr and many other dispersion strengthened materials.

As anticipated by Shewfelt and Brown,[88] there are also serious objections that can be raised against the basic assumption of 'local' climb. The postulate concerning dislocation shape in the vicinity of the dispersoid particle must be regarded as unduly restrictive. Lagneborg[94] has argued that local climb would be an extreme non-equilibrium process: the sharp bend in the dislocation at the point where it leaves the particle–matrix interface will in reality be rapidly relaxed by diffusion, leading to more 'general' climb. Because the additional line length then required depends on the kinetics, a 'back stress' is predicted which scales as the applied stress. This would result only in a retardation of creep, with the same stress exponent as for the particle-free material (see eqn (5) with $\sigma_0 \sim \sigma$); such behaviour would clearly be in contradiction to experimental data on dispersion strengthened materials. In addition, as discussed by Rösler,[66] there appears to be a flaw in the calculations, leading to gross overestimation of the diffusive fluxes.

In the meantime it has become clear that a finite but small threshold stress must always exist: in order to thread over and under dispersoid particles in a random arrangement, a small elongation of the dislocation line is inevitable. The resulting threshold stress for 'general climb' over

spherical particles is given by[88,92,95]

$$\sigma_{th} = \sqrt{\frac{3f_V}{2\pi}}\,\sigma_{Or} \tag{11}$$

which results in negligible numerical values (less than 10% of the Orowan stress) for low volume fractions up to 10%. When a random particle distribution is assumed[92] and when Friedel statistics are applied[14] these values are further reduced to less than about 2%. In conclusion, it can be said that climb-related threshold stresses are sensitive to the details of the climb process especially in one regard: the degree to which climb is localized at the particles.

In order to solve the long-standing problem of climb localization, Rösler and Arzt[96] have considered the kinetics of dislocation climb over cuboidal particles. The only assumption concerning the dislocation geometry was that of local equilibrium (Fig. 15(b)): the chemical potential for vacancies along segment BD (where it is lowered by the curvature) is set equal to the chemical potential along AB (where it is negatively biased by the applied stress). Local equilibrium can be assumed to form rapidly by short-range diffusion, while the supply of new vacancies for climb and dislocation advance typically requires diffusion over the distance of one particle spacing. This leads to a more natural dislocation configuration for which the diffusion kinetics are then evaluated.

The resulting constitutive equation for 'equilibrium climb' does not contain any adjustable parameters:

$$\dot{\varepsilon} = \frac{\rho G b^4 B}{k_B T d^3}\left(a_p D_p + \pi D_V l d\right)\left(\frac{\sigma - \sigma_{th}^r}{\sigma_{Or}}\right)^n \tag{12}$$

where

$$B = 60 \times 10^{-1{\cdot}9\beta}(d/h)^{1{\cdot}6}$$

$$n = 3{\cdot}5\,\beta^{0{\cdot}3}(h/d)^{0{\cdot}2}$$

$$\sigma_{th}^r = \sigma_{Or}\sin\left(\frac{2h}{l}\tan\beta\right)$$

Here ρ is the density of mobile dislocations, d, h and β are particle width, height and angle according to Fig. 15(b), l is the particle spacing, $a_p D_p$ is the cross-section of a dislocation core times its diffusivity, D_V is the volume diffusivity, σ the applied stress, σ_{th}^r a threshold stress for 'general' climb and σ_{Or} the Orowan stress.

An important result which emerges from this treatment of 'equilibrium climb' is that truly 'local' climb is always unstable, although the extent to which climb is localized in the vicinity of the dispersoid

particle increases with applied stress. This implies that the number of vacancies required for climb (which is proportional to the length of the climbing segment) decreases as the stress increases, and therefore the dislocation velocity depends over-linearly on stress. The maximum climb-related stress exponents predicted by this model ($n \approx 6$) are, however, far below the values typical of dispersion strengthened materials. We note in passing that 'equilibrium climb' offers a good qualitative explanation for the (much less stress-sensitive) creep behaviour of materials with coherent precipitate particles. There the climb process seems to be dominant at high temperatures (for a review see, e.g., Ref. 14).

In summary, it seems that the assumption of dislocation climb alone cannot explain the high stress sensitivity for creep in dispersion strengthened materials. In other words, if the only effect of dispersoid particles consisted in forcing the dislocations to climb over them, they would be weak barriers to slow creep deformation at high temperatures. Several authors have endorsed the conclusion that the 'threshold stresses' in dispersion strengthened alloys can probably not be attributed to the dispersoids acting merely as obstacles to dislocation climb.[14,95] Climb models will be further discussed and assessed in Section 3.4.

3.2 Particle–dislocation interaction: experimental observations

In the search for a genuine threshold stress mechanism, attention has only recently turned to the details of the possible interactions between dispersoids and hard particles. Much insight has been gained by transmission electron microscopy of the dispersoid–dislocation configurations in creep-exposed specimens of dispersion strengthened alloys.[97–100,65,66] It is generally observed that the dislocation distribution is quite inhomogeneous, which points to unstable deformation. In the vicinity of the 'threshold stress', single dislocations are seen to interact with single dispersoids. Only at higher stresses, where the alloys approach the behaviour of the dispersoid-free matrix, have dislocation substructures been reported.[65]

The most detailed study to date has been conducted on the ODS superalloy MA 6000, which was creep-deformed at temperatures near 1000 °C and under stresses well below the Orowan stress. A typical micrograph, taken subsequently under 'weak-beam' conditions by Schröder,[100] is shown in Fig. 17(a). The dislocation is seen in a situation where it has already surmounted a dispersoid by climb and adheres to

(a)

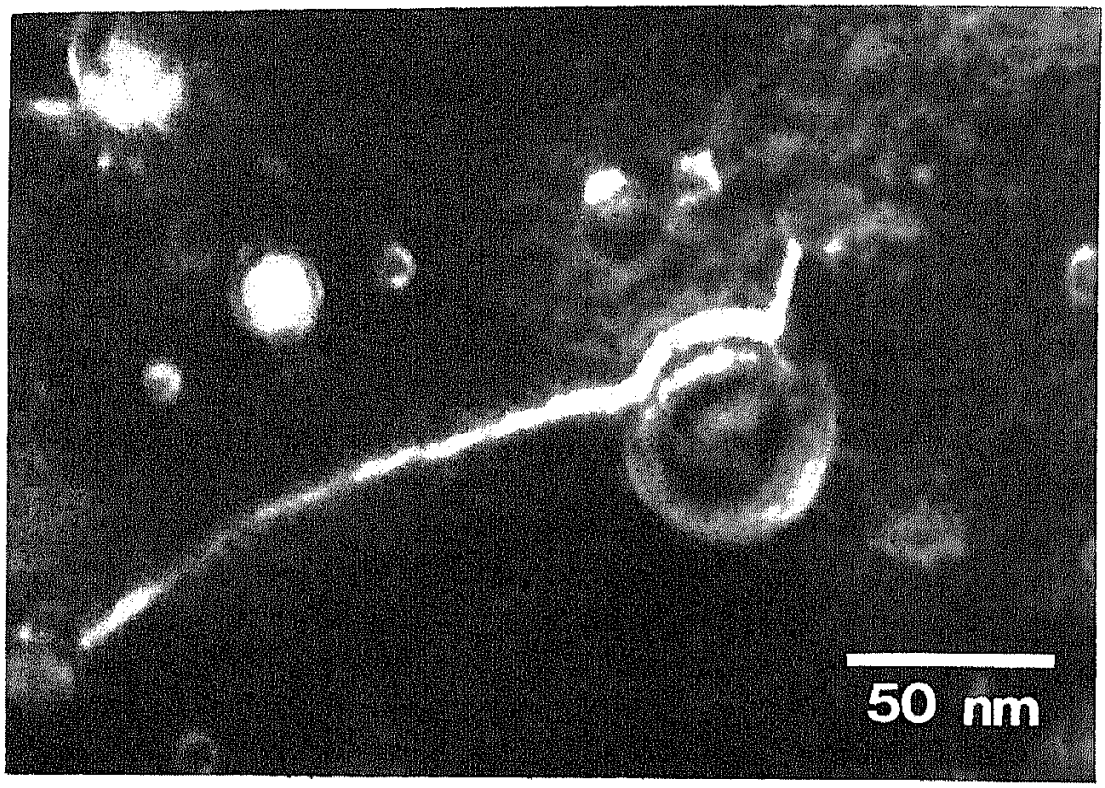

(b)

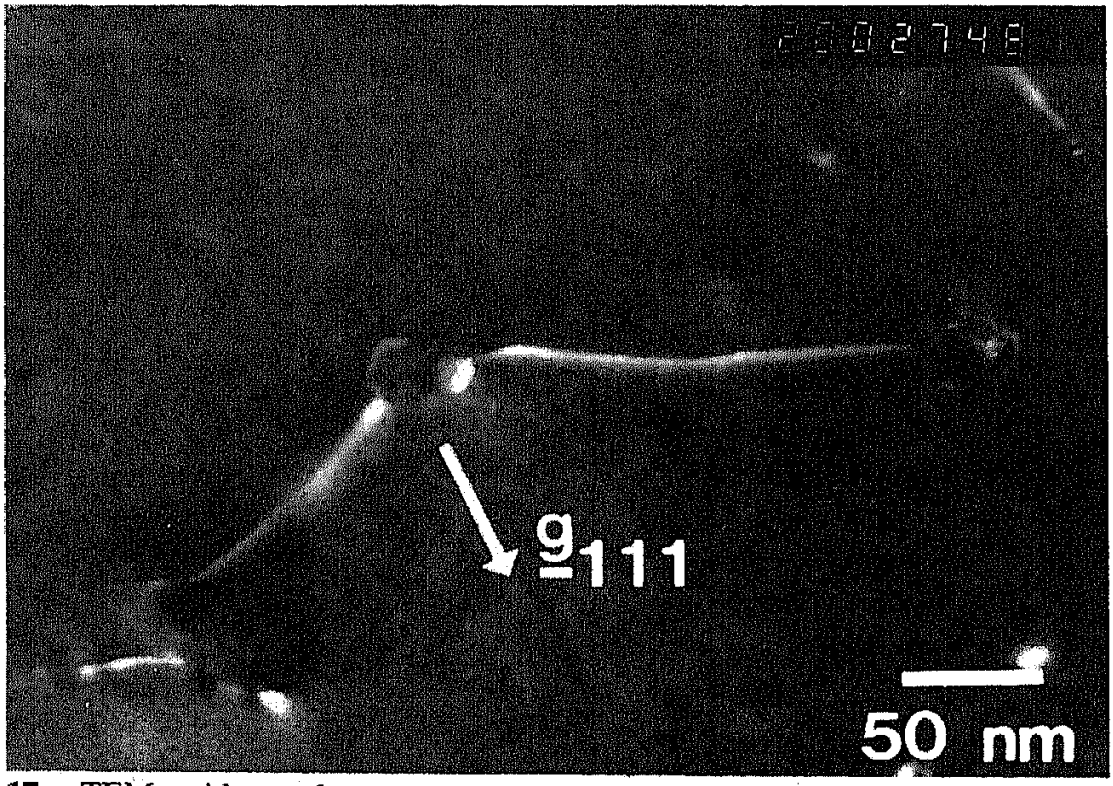

Fig. 17. TEM evidence for an attractive dislocation–dispersoid interaction during creep: (a) in Inconel MA 6000 (Ref.100); (b) in Al–Al_2O_3 (Ref. 66); (c) in SiC–B_4C (Ref. 101).

(a)

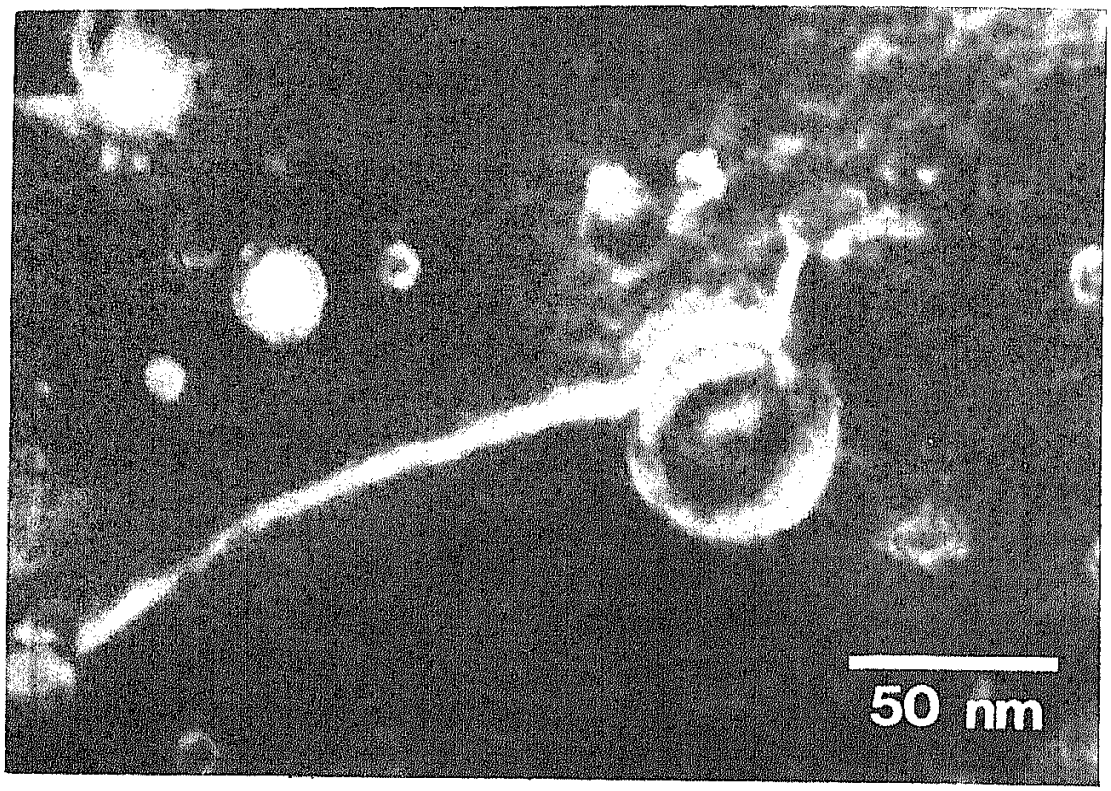

(b)

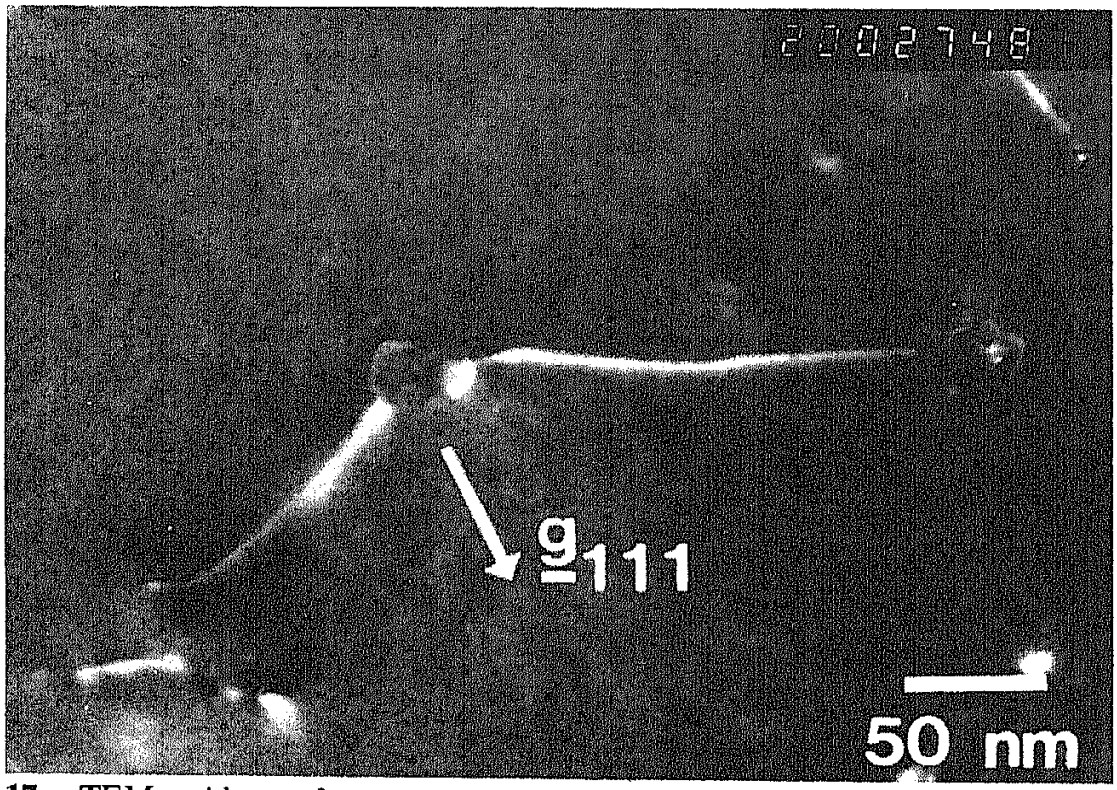

Fig. 17. TEM evidence for an attractive dislocation–dispersoid interaction during creep: (a) in Inconel MA 6000 (Ref.100); (b) in Al–Al_2O_3 (Ref. 66); (c) in SiC–B_4C (Ref. 101).

(c)

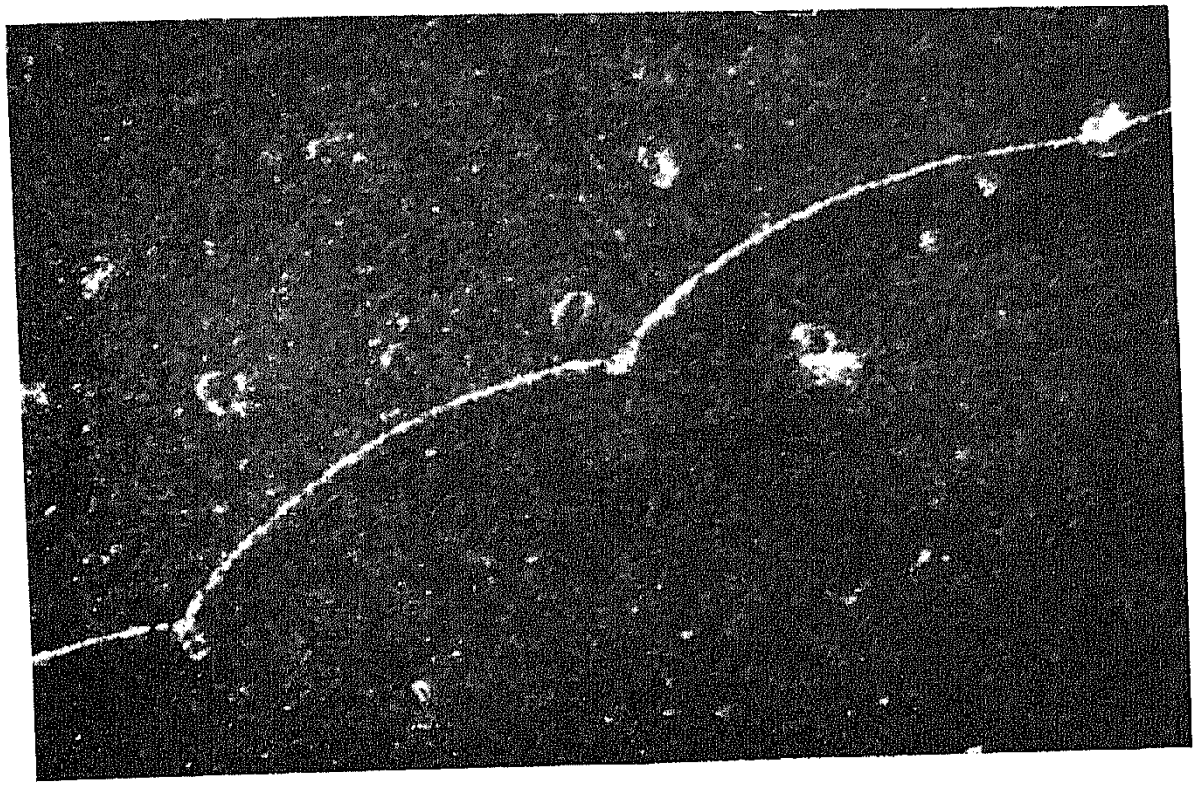

Fig. 17—*contd.*

the 'departure side' of the dispersoid. Under 'weak-beam' conditions, the contrast of the dislocation segment which resides in or near the dispersoid–matrix interface is often well visible. This feature of dislocation detachment has been found on more than 100 similar micrographs, and much care was taken to exclude artefacts related to experimental procedures and electron contrast. A cut-off in dispersoid size was found ($d \approx 15$ nm), below which dislocations were no longer seen to adhere to the particle–matrix interface. To decrease the likelihood of effects related to thermal misfit, in-situ heating experiments were conducted which gave the same dislocation configurations.

Similar but less detailed observations were reported in the dispersion strengthened NiCr alloy MA 754 by Nardone and Tien,[97] who were the first to point out the possibility of pinning on the 'departure-side', and in dispersion strengthened Al by Rösler[66] (Fig. 17(b)). Possible indications for a detachment mechanism under conditions of power-law creep have also been found in a SiC ceramic containing dispersoids of B_4C (Fig. 17(c), Davis and Posthill[101]). Circumstantial evidence for an attractive interaction between dislocations and dispersoids has previously been reported for K-bubble strengthened tungsten,[77] a dispersion strengthened Al–Li alloy[102] and the aluminium alloy IN 9052 (Ref. 59).

(c)

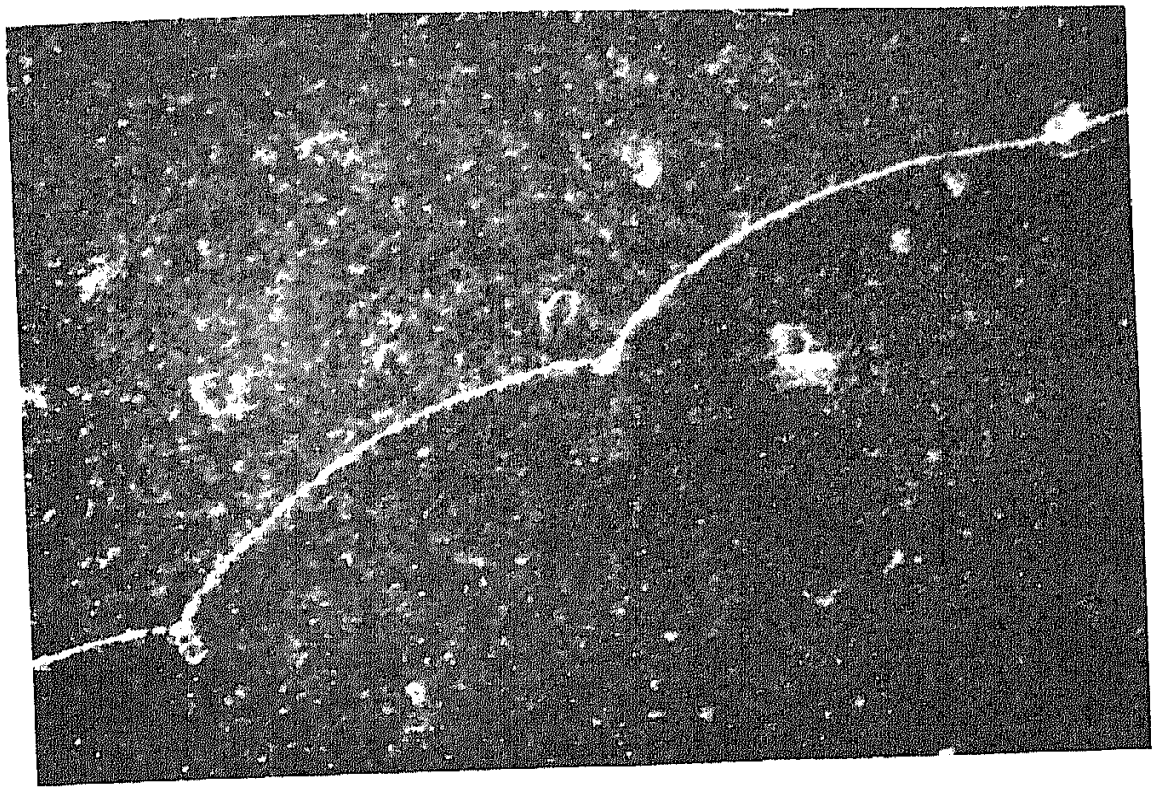

Fig. 17—*contd*.

the 'departure side' of the dispersoid. Under 'weak-beam' conditions, the contrast of the dislocation segment which resides in or near the dispersoid–matrix interface is often well visible. This feature of dislocation detachment has been found on more than 100 similar micrographs, and much care was taken to exclude artefacts related to experimental procedures and electron contrast. A cut-off in dispersoid size was found ($d \approx 15$ nm), below which dislocations were no longer seen to adhere to the particle–matrix interface. To decrease the likelihood of effects related to thermal misfit, in-situ heating experiments were conducted which gave the same dislocation configurations.

Similar but less detailed observations were reported in the dispersion strengthened NiCr alloy MA 754 by Nardone and Tien,[97] who were the first to point out the possibility of pinning on the 'departure-side', and in dispersion strengthened Al by Rösler[66] (Fig. 17(b)). Possible indications for a detachment mechanism under conditions of power-law creep have also been found in a SiC ceramic containing dispersoids of B_4C (Fig. 17(c), Davis and Posthill[101]). Circumstantial evidence for an attractive interaction between dislocations and dispersoids has previously been reported for K-bubble strengthened tungsten,[77] a dispersion strengthened Al–Li alloy[102] and the aluminium alloy IN 9052 (Ref. 59).

While these TEM studies by no means constitute unambiguous proof, they strongly suggest a new dislocation mechanism: particle bypassing by climbing dislocations may not be controlled by the climb process (as postulated in the early threshold stress models), but by a resistance to dislocation detachment from the particle. In other words, 'threshold stresses' for creep would have to be attributed to an attractive particle–dislocation interaction. Supporting theoretical evidence suggests that this is not unreasonable, as will be shown below.

3.3 Particle–dislocation interaction: mechanistic models

Recent theoretical analysis indeed confirms that the assumption of an attractive particle–dislocation interaction at high temperatures can be justified. Srolovitz *et al.*[103–106] have solved the elastic problem of an edge dislocation interacting with a cylindrical particle, subject to the boundary conditions that both tangential tractions and gradients in the normal tractions at the particle–matrix interface are instantaneously relaxed. Such relaxation processes can be accomplished at elevated temperatures by boundary and volume diffusion, and by sliding of the phase boundary. Calculation of the characteristic relaxation times using equations by Mori *et al.*[107] suggests that relaxation, at least of deviatoric stresses, will indeed occur quickly; therefore the dispersoid can be treated as a void (with an internal pressure corresponding to the hydrostatic component of the applied stress). The Srolovitz solutions show that at high temperatures the elastic interactions between dispersoids and dislocations become unimportant: even an infinitely stiff particle (which repels dislocations at low temperatures) can produce a strong attractive force, provided it is not coherent with the matrix.

Srolovitz *et al.*[105] further conclude from an evaluation of the glide and climb forces acting on the dislocation, that it will always end its trajectory in the particle–maxtrix interface, without being able to climb over the particle. It is further suggested that core delocalization will occur in the interface. Therefore, the unpinning stress should be similar to that for voids, i.e. approximately equal to the Orowan stress.[108]

There appears to be, however, an important discrepancy of these predictions with some TEM observations. The 'weak-beam' micrograph in Fig. 17(a) shows clearly that the identity of the dislocation is preserved in the vicinity of the particle–matrix interface and the local strain is not noticeably reduced by core spreading. Contrary to the behaviour of a void, the dispersoid evidently allows only a modest relaxation of the dislocation. That the detachment threshold can act as the decisive dislocation barrier even at small degrees of relaxation has

been established by Arzt and Wilkinson.[109] They treat the effects of an attractive interaction on the energetics of dislocation climb. In their model a variable attractive interaction is introduced by assigning a line tension to the dislocation segment at the particle which is lowered by a factor $k(k<1)$. This parameter describes the extent to which the dislocation relaxes its energy by interaction with the particle–matrix interface. For $k=1$, no relaxation and, thus, no attractive interaction occurs; $k=0$ signifies maximum interaction which is approximately realized by the presence of a void. This approach clearly excludes long-range attractive forces between particles and dislocations.

The authors have calculated force–distance profiles for local climb under the action of different attractive forces. The main result is that an attractive interaction causes a significant threshold stress which must be exceeded in order to detach the dislocation from the back of the particle and which is given by

$$\sigma_d = \sqrt{1-k^2}\,\sigma_{Or} \tag{13}$$

This 'detachment threshold' is independent of the shape of the particle and its position with respect to the glide plane. It applies regardless of the details of the climb process which precedes detachment. Therefore the result is formally identical with the strength due to coherent, shearable particles with a lower modulus (by the factor k) than the matrix.[110]

Because of the reduced line tension of the dislocation segment at the dispersoid, the 'threshold stress' for local climb is lowered. In Fig. 18, the detachment threshold is compared with the threshold for local climb as a function of k. Although we now know that the latter is probably an overestimate of the climb threshold (see Section 3.1), the position where the two curves intersect illustrates an essential point: only a very modest attractive interaction, corresponding to a relaxation of about 6% ($k\approx 0{\cdot}94$), is required in order for dislocation detachment to become the event which controls the threshold stress. If general climb with its much smaller threshold stress were considered, the transition point would be shifted to $k\approx 1$ and the relaxation required for 'detachment control' would be even more negligible. Because, in view of Srolovitz's calculations, some relaxation will always occur at the interface, these results lend strong support to the detachment process as a serious candidate for a 'threshold stress' mechanism.

Recently, a full kinetic model for dislocation climb which allows for the effects of an attractive interaction has been developed by Arzt and Rösler.[111] The results show that an attractive interaction may in fact stabilize 'local' climb over cuboidal particles at sufficiently high stresses,

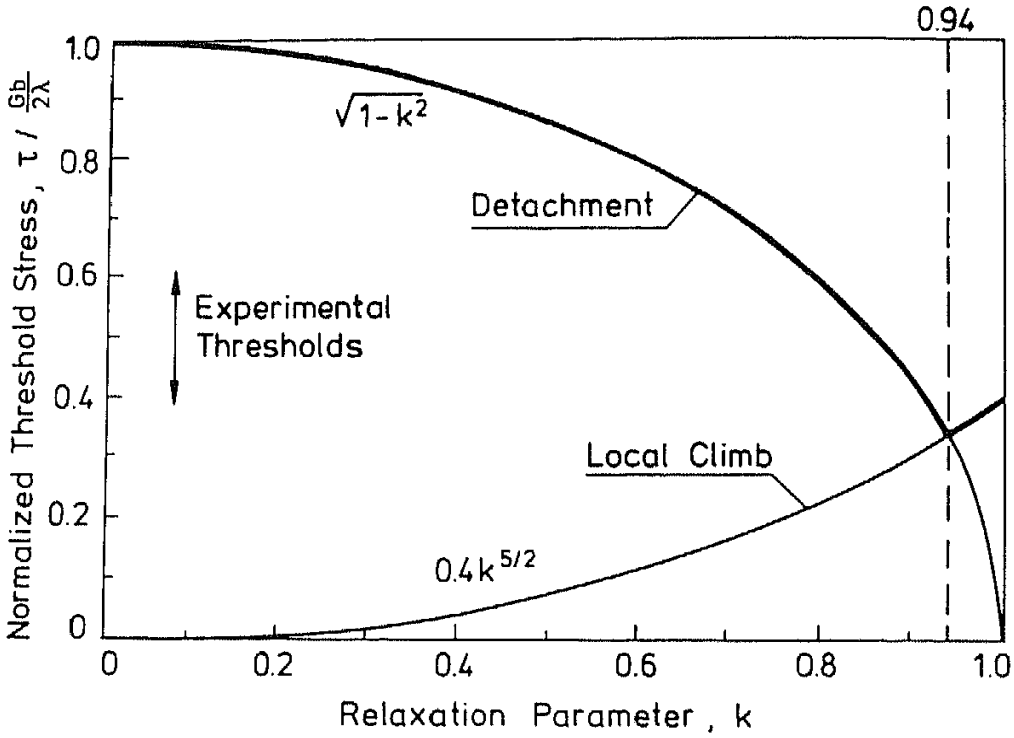

Fig. 18. Theoretical threshold stresses for local climb over spherical dispersoids and for dislocation detachment, as a function of the strength of the dislocation–dispersoid attraction (relaxation factor k) (from Ref. 109). The attractive interaction increases from right to left on the abscissa.

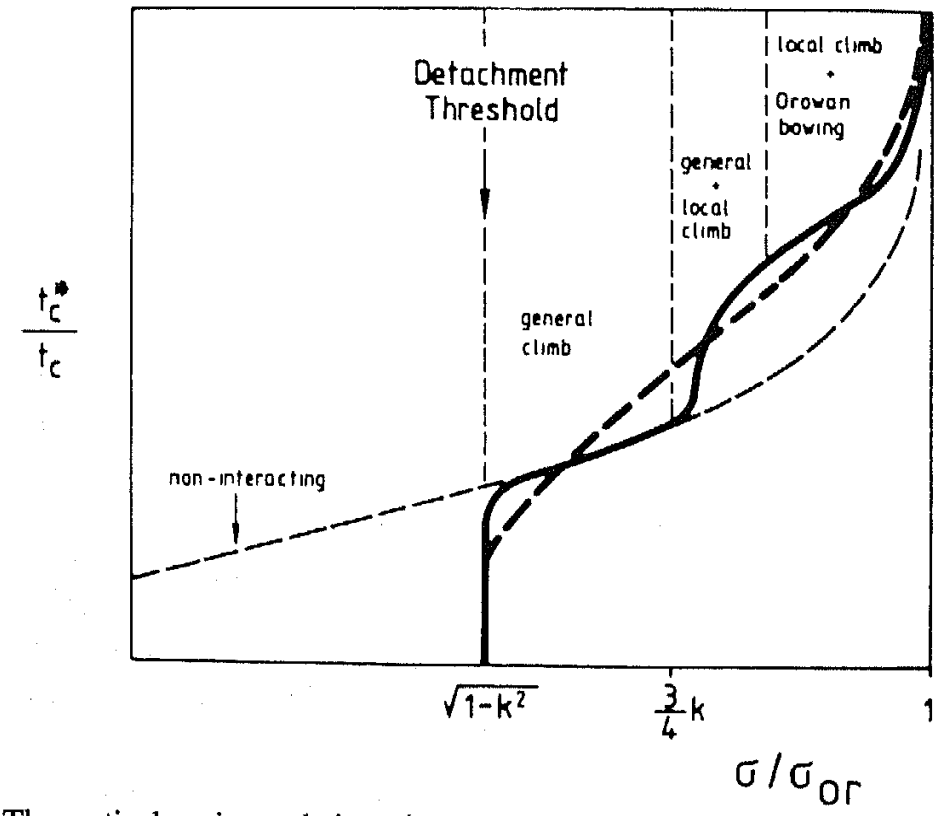

Fig. 19. Theoretical reciprocal time (normalized) for a dislocation to climb over and detach from a cuboidal, attractive dispersoid, as a function of the stress divided by the Orowan stress. The prevailing climb geometry is indicated. For comparison, the result for 'non-interacting' (non-attractive) dispersoids is also included (from Ref. 111),

i.e. for $\sigma > \frac{3}{4}k\,\sigma_{Or}$ for $\beta = 45°$ (Fig. 19). The creep behaviour of alloys with attractive particles, however, is always dominated by the detachment threshold. The 'oscillations' in Fig. 19 were attributed to the unrealistic simple particle shape, which must be adopted to make the problem tractable.

The extremely sharp threshold behaviour in Fig. 19 can be remedied by considering thermal activation of dislocation detachment from particles. This aspect has been analysed in detail by Rösler[66] and Rösler and Arzt.[112] An approximate expression for the activation energy for dislocation detachment, as a function of particle radius r, interaction factor k and normalized applied stress σ/σ_d was derived on the basis of the model by Arzt and Wilkinson.[109] The resulting constitutive equation for 'detachment-controlled creep' is given by

$$\dot{\varepsilon} = \dot{\varepsilon}_0 \exp\left[-\frac{Gb^2r}{k_BT}(1-k)^{3/2}\left(1-\frac{\sigma}{\sigma_d}\right)^{3/2}\right] \tag{14}$$

where $\dot{\varepsilon}_0 = CD_V l\rho/2b$ and σ_d is given by eqn (13).

For random arrays of attractive particles, computer simulations have shown that the same kind of law is retained.[91] Equation (14) is plotted in Fig. 20 for different values of k. Several features which are in qualitative agreement with experimental results can be identified: dispersoids with a strong attractive interaction ($k < 0{\cdot}85$) do indeed produce a region of high stress exponent which extends over many orders of magnitude in strain rate; this gives the appearance of a 'threshold stress', which falls with increasing temperature. As the interaction gets weaker (or, equivalently, if the temperature is raised), a concave curvature at low stresses becomes apparent; this corresponds to a loss of strength which would not be expected by linear extrapolation of the data from higher strain rates. It is also clear from Fig. 20 that there is no 'universal' stress exponent for dispersion strengthened materials; rather the stress sensitivity depends on temperature, stress and dislocation–dispersoid interaction.

When the interaction parameter k and the pre-exponential factor are adjusted, eqn (14) can be made to describe the creep behaviour of several dispersion strengthened materials extremely well. An example is shown in Fig. 21 for the dispersion strengthened aluminium alloy AlC2. Both the high stress sensitivity and the temperature dependence are quantitatively explained with the model when a temperature-independent value is assigned to k ($k = 0{\cdot}75$). Similar agreement is found for Ni base, and other Al base dispersion strengthened materials.[66] The interaction factors for different dispersoids, obtained by fitting the theory to the data, are listed in Table 2.

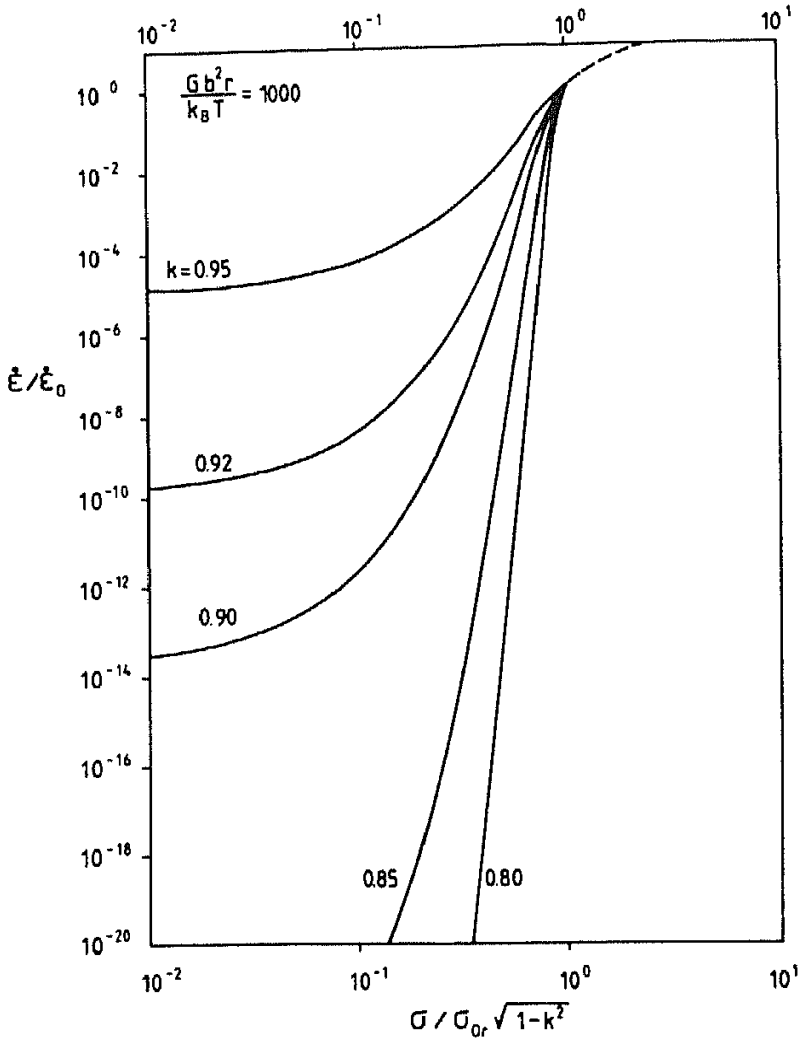

Fig. 20. Theoretical prediction of the creep rate (normalized) as a function of stress (normalized) on the basis of thermally activated dislocation detachment from attractive dispersoids (eqn (14)), as a function of interaction parameter k. The change of curvature at high strain rates (broken line) indicates the transition to the creep behaviour of dispersoid-free material and does not follow from the equation (from Ref. 112).

It is seen that k varies characteristically with the type of dispersoid: besides the K-bubbles in tungsten, carbides in aluminium seem to be most efficient in attracting dislocations, while oxides appear less suitable. A particularly instructive example is the rapidly solidified Al–Fe–Ce alloy studied by Yaney *et al.*[71] Its 'anomalous' creep behaviour can be fully described by assigning a weak interaction effect ($k = 0{\cdot}95$), again independent of temperature, to the intermetallic precipitates (Fig. 22). This interpretation is also consistent with Yaney *et al.*[71] who have shown that the loss of strength at higher temperatures cannot be attributed to thermal instability of the microstructure.

Finally, an optimum dispersoid size, for a given volume fraction, is predicted by this model, as the activation energy in eqn (14) goes through a maximum as a function of dispersoid size. Physically, this

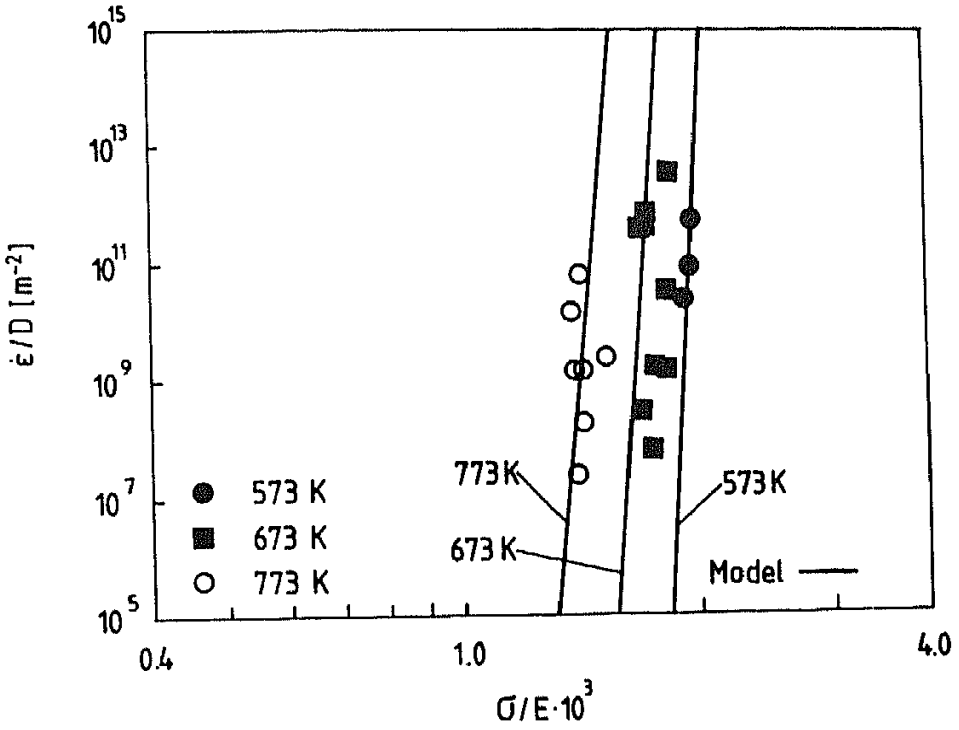

Fig. 21. Experimental creep data for Al–Al_4C_2, Al_2O_3 (alloy AlC2, symbols) and theoretical predictions from the detachment model with $k = 0{\cdot}75$ (lines) (from Ref. 66).

comes about because (i) the probability of thermally activated detachment is raised for small dispersoids, and (ii) large particles are associated, at given volume fraction, with a low Orowan stress and hence a small athermal detachment stress σ_d. The prediction of an optimum dispersoid size would be in qualitative agreement with TEM observations which show that dislocations do not adhere to very small dispersoids,[37,100] and with experimental results of Benjamin[113] to the effect that coarsening of dispersoids results in a much smaller reduction of creep strength than would be expected on the basis of the Orowan model. Obviously, additional experiments must be conducted to test

TABLE 2

Interaction Parameter k for Different Materials, Determined by Fitting Eqn (14) to Experimental Creep Data (Ref. 66)

Material	*Reference*	*Dispersoid*	k
AlC2	65, 66	$Al_2O_3 + Al_4C_3$	0·75
AlC0	65, 66	Al_2O_3	0·84
AlMg4C1	65, 66	$MgO + Al_4C_3$	0·85
Al–Fe–V–Si	72	$Al_{12}(Fe,V)_3Si$,. . .	0·93
Al–Fe–Ce	71	intermetallic	0·95
MA 6000	125	Y_2O_3	0·92
W–K	76, 77	K-bubbles	0·78

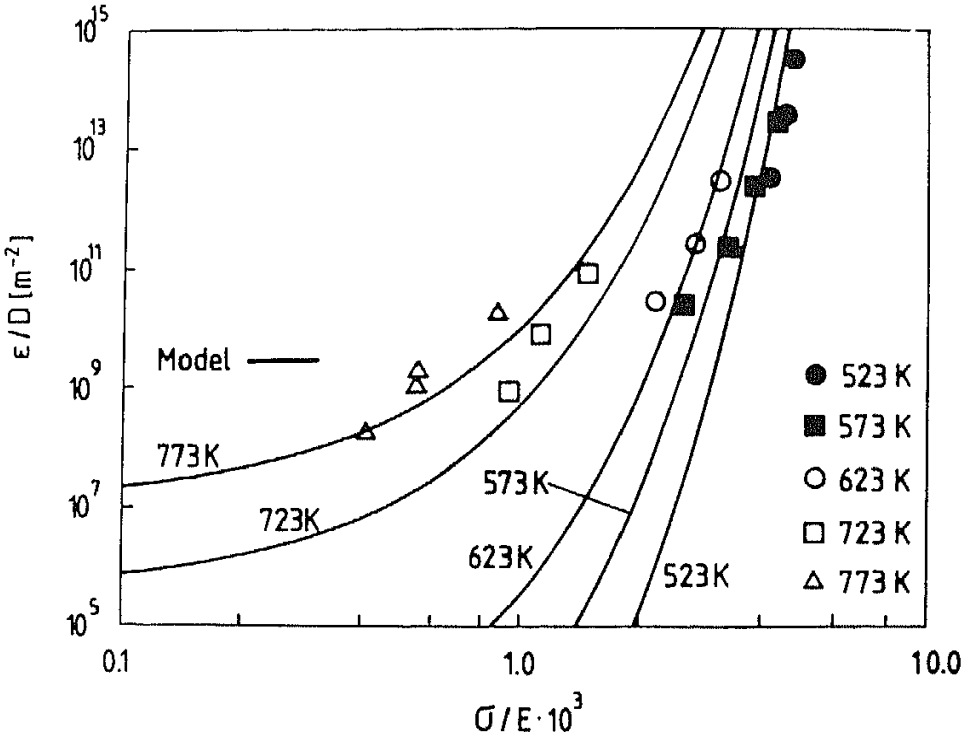

Fig. 22. Experimental creep data for an Al–Fe–Ce alloy (non-MA variant) strengthened by intermetallic precipitates (symbols, Ref. 71) and theoretical predictions from the detachment model with $k = 0{\cdot}95$ (lines) (from Ref. 66).

these predictions and to critically examine the validity of this new concept of 'detachment-controlled creep'.

3.4 Discussion of the creep models

The state of the theory of dispersion strengthening at high temperatures can be summarized as follows. Essentially two types of mechanistic models for the effect of dispersoid particles on creep have been proposed: (i) 'climb models' based on the assumption that climb of dislocations over dispersoids controls the creep rate, and (ii) 'detachment models' which attribute the decisive dispersoid effect to an attractive interaction with dislocations. Both concepts agree that climb must be occurring. They have also reached a similar level of sophistication: the interaction of one dislocation with a dispersoid or an array of dispersoids is treated in the line-tension approximation. Calculations which incorporate the self-stress of the bowed-out dislocation segments have not been reported, but comparison with available results for Orowan bowing[114,115] indicate that the dispersoids are probably too weak obstacles at high temperatures for the 'dipole interaction' to become important.[91] Detailed calculations would, however, be desirable.

Also both concepts neglect the possible effects of dislocation substructures.[16,95,116] According to TEM results, these are probably not important in the vicinity of the 'threshold stress' but may become decisive well above the 'threshold stress'. This may be the reason for an inability of both concepts to describe the data in that region (region I in Fig. 13). At such high strain rates, which, however, are less interesting from an application point of view, a combination with the creep law for the dispersoid-free matrix will be necessary.

The differences between the 'climb models' and the 'detachment models' are manifold. The Shewfelt–Brown equation (eqn (10)) for 'local climb' is impressive because it is, at least in principle, fully predictive without any adjustable parameters. In practice it seems that both a pre-factor and the Orowan stress, which is usually difficult to calculate for complex materials to any acceptable degree of accuracy, must be adjusted to give agreement with experimental results. The Rösler–Arzt equation (eqn (14)) for 'detachment-controlled creep' contains one additional parameter, i.e. the relaxation parameter k. It comes as no surprise that introduction of this parameter leads to better agreement with a given set of experimental data. Because of inevitable experimental scatter, it is difficult to decide on the quality of fit which equation should be preferred; instead, one must invoke physical plausibility.

The following arguments tend to give an important edge to 'detachment models':

—For several types of dispersoid, the assumption of detachment control explains both the stress dependence and the temperature dependence of the creep rate. As has been shown in the previous section, even the 'abnormal' loss of strength of rapidly solidified alloys at high temperatures can be quantitatively accounted for by setting the relaxation parameter to a fixed (temperature-independent) value. The concept can also explain high stress exponents which are approximately constant over several orders of magnitude in strain rate (see Fig. 20), as has been found experimentally for mechanically alloyed materials.

—The relaxation parameter k has a well-defined physical meaning and is not merely a fitting constant. Its values are physical reasonable (i.e. in the range of dislocation core energies), vary characteristically with the type of dispersoid, and are independent of temperature (as suggested by the short relaxation times, *cf.* Section 3.3). Through this factor, high temperature strength is decoupled from room temperature strength (for dispersoids with a

weak interaction effect); 'climb models' would predict a constant ratio of creep strength over Orowan stress and thus cannot explain the loss of strength, at high temperatures, in materials with fairly stable dispersoids.

—Finally, a point of physical justification: the only convincing argument for the peculiar geometry of 'local' climb can be the existence of an attractive dislocation–dispersoid interaction.[111] Even a small interaction, however, is sufficient for detachment to dominate the bypass process, has been shown by Arzt and Wilkinson.[109] Further, 'detachment control' is consistent with TEM observations which suggest an attractive dislocation–dispersoid interaction.

On the other hand, there are several questions which need to be tackled in order to lend further support to the concept of detachment control:

—Most importantly, the physics of the interaction between dislocations and particles at high temperatures are insufficiently understood. While it seems intuitively reasonable that incoherent dispersoids would allow a higher degree of dislocation relaxation than coherent particles, the connection of relaxation with the atomic structure of the phase boundary is not yet understood. It is plausible that the value of k may depend not only on the nature of this interface but also, for example, on particle size.

—No definite microstructural proof of a detachment mechanism has been given to date, as 'post-mortem' TEM studies inevitably bear some residual risk of artefacts. In-situ TEM deformation experiment might provide valuable insight.

—As discussed by Rösler and Arzt,[112] the necessity of fitting the pre-exponential factor in eqn (14) is still unsatisfactory. Also the convex curvature of $\log \dot{\varepsilon}$–$\log \sigma$, which is often reported, cannot be reproduced. Further critical data analysis in terms of the model will be necessary in order to substantiate the promises of this concept.

On the basis of the assumed validity of 'detachment control', several conclusions can be drawn, some of which must necessarily remain speculative at the present state. Above all, the 'threshold stress' concept, when applied uncritically, can be seriously misleading. Contrary to the implications of the 'local climb' models, *there exists no significant minimum 'threshold stress'* (apart from a small threshold for 'general' climb) that must be exceeded in order to sustain creep deformation. Laboratory creep rates may indeed give the impression of

a 'threshold stress' behaviour but eventually, at sufficiently low strain rates, an upward curvature of the $\dot{\varepsilon} - \sigma$ curves is inevitable. The model thus offers an additional explanation for the 'Region III' in Fig. 13, even for single crystals with thermally stable dispersoids. Until now such a loss of strength has been attributed alternatively to the dissolution, coarsening or deformability of dispersoid particles (in TD–NiCr single crystals[25] and in Al[58]) or to the onset of grain boundary sliding or damage formation (MA 754[29] and Al[65]).

For the purpose of lifetime prediction, it must be realized that extrapolations from laboratory data to low creep rates can be seriously in error. Only materials with highly attractive dispersoids ($k < 0{\cdot}8$) would permit linear extrapolation. The value of k, which is therefore important, can be estimated, by a method proposed by Rösler,[66] from the values of the apparent stress exponent and the apparent activation energy for creep. In conclusions, even in cases where near–'threshold stress' behaviour is observed, it seems warranted, in the interest of clarity, to use the term 'pseudo-threshold' instead.

The practical perspectives in terms of alloys design are enticing but still vague. Given a certain usable volume fraction of dispersoid (which is limited by minimum ductility requirements), the 'detachment model' predicts that there should be an optimum particle size (and spacing), while 'climb models' demand a small spacing (the radius enters only in the kinetics). Furthermore, 'detachment' discriminates different dispersoids by the degree of dislocation relaxation, suggesting that the properties of the dispersoid–matrix interface should be of critical importance. Interestingly, Table 2 suggests tentatively that particles dispersed by mechanical alloying tend to be more efficient than those produced by (rapid) solidification. It remains to be seen whether concepts such as interface modification by segregation alloying can be put to use in order to further improve the efficiency of dispersoids.

4 FURTHER CONSIDERATION: GRAIN BOUNDARY EFFECTS ON CREEP DEFORMATION AND FRACTURE

The previous considerations, which concerned the role of dispersoid particles in impeding the motion of lattice dislocations, can be strictly valid only for single crystals, in which grain boundaries do not contribute to creep deformation. Grain boundary weakening is of particular importance for polycrystalline dispersion strengthened materials which as engineering materials are subjected to moderate stresses at high homologous temperatures. Under these conditions grain boundaries

become weak microstructural elements which can impair the mechanical properties substantially (see, e.g., Figs 3, 5, 6 and 11). This is particularly true for dispersion strengthened systems, where the strength differential between grain interiors and grain boundaries is high. Because of processing limitations, single crystals of dispersion strengthened materials are difficult, if not impossible, to produce in useful dimensions. Therefore the effects of grain boundaries on deformation and fracture have received considerable attention in the literature; the understanding is, however, still incomplete.

In general, grain boundaries can lower the high-temperature strength in at least three ways: (i) stress-induced vacancy accumulation leads to cavity formation on grain boundaries transverse to an applied tensile stress and, subsequently, to premature intergranular failure; (ii) grain boundary sliding results in stress concentrations which accelerate dislocation creep; and (iii) by acting as vacancy sinks and sources, grain boundaries promote additional grain deformation due to diffusional creep ('Nabarro–Herring creep'). All of these processes are influenced by the presence of dispersoid particles.

Models for the growth of creep cavities in elongated grain structures typical of some modern dispersion strengthened materials have been developed by Arzt,[117] Arzt and Singer,[35] Stephens and Nix,[118] and Zeizinger and Arzt.[36] In view of the high resistance to dislocation creep, all models assume pore growth to occur by diffusion; this is supported by observations of particle-free zones in the ligaments between creep cavities.[118,36] The theories differ in the type of accomodation process necessary for assuring compatibility between the deformation of damaged and undamaged grains. When sliding along longitudinal grain boundaries provides sufficient accomodation, the strain rate due to cavity growth can be expressed as [117,35]

$$\dot{\varepsilon} = \frac{C\delta D_b \Omega}{kTh^2 L} \cdot \frac{\sigma - \sigma_0 - 2\tau_0 R}{\lambda^2/h^2 + 2R} \tag{15}$$

where R is the grain aspect ratio ($=L/l$ with L and l the long and short grain dimensions, respectively), h the height of grain boundary serrations, Ω the atomic volume and λ the cavity spacing. As suggested earlier by Brown,[11] a dependence on the grain aspect ratio arises naturally in this model from the coupling of grain boundary sliding and cavity growth, between which the applied stress is distributed. A shortcoming of this approach is the linear stress dependence of the creep rate; only by assuming finite values of threshold stresses for cavity formation (σ_0) and/or for grain boundary sliding (τ_0) was it possible to obtain quantitative agreement with the experimental rupture times on MA 6000

(Fig. 5). Also, sliding could not be detected in model experiments by Zeizinger and Arzt,[36] which casts some doubt on the applicability of the model to alloys like MA 6000.

A similar model was proposed by Stephens and Nix,[118] who report fine-grain pockets along the longitudinal boundaries of coarse elongated grains in one heat of MA 754. By attributing the accommodation to diffusional creep of these pockets, they arrive at the following result:

$$\dot{\varepsilon} = \frac{80 D_V w \Omega}{kTd^2 L} \cdot \frac{\sigma - (1-f)\sigma_{cs}}{10\pi\lambda w K/d^2 + R} \tag{16}$$

where d is the size of the fine grains, L the length of the coarse grains, f the fraction of cavitated boundary area, σ_{cs} the cavity sintering stress, w the width of fine-grain pockets and K an f-dependent parameter. This equation again predicts a linear stress dependence, which is in good agreement with experimental results (Fig. 3(a), 'heat 2'). Only an approximately linear increase in rupture strength with grain aspect ratio is predicted, while the cavity half-spacing λ is found to be a much more decisive (though less variable) parameter for rupture strength.

Another possibility for damage accommodation is by dislocation creep, enhanced by the shedding of load from cavitating grain boundaries to the adjacent intact grains. A numerical solution for this case by Stephens and Nix[118] gives a strong dependence of the rupture time on GAR. The experimental strain-rate/stress dependence of MA 754 with uniform fibre grain morphology ('heat 1') is well described by this model, except at low stresses where creep strength is consistently overestimated. Zeizinger and Arzt[36] take a similar modelling approach which yields the following analytical equation for the rupture time:

$$t_f = \frac{0{\cdot}085 k_B T \lambda^3}{\delta D_b \Omega \sigma}\left[1 - \left(1 - \frac{1}{R}\right)^n\right] + \frac{\varepsilon_B}{\dot{\varepsilon}_u}\left(1 - \frac{1}{R}\right)^n \tag{17}$$

where ε_B is the total strain due to void growth and $\dot{\varepsilon}_u$ the creep rate of uncavitated material. This equation, which was derived on the basis of a model by Cocks and Ashby[119] for equiaxed grains, is found to describe the GAR-dependence of the rupture time in MA 6000 (Fig. 5) well. Also the poor rupture properties in the transverse direction can be understood because a low GAR applies in this case. It is to be expected, however, that at low GAR eqn (17) underestimates the stress dependence of the rupture time, as discussed Zeizinger and Arzt.[36]

In the light of these investigations it appears that the GAR-dependent 'threshold stresses for diffusional creep' reported by Whittenberger[42] (see Section 2.1.1) could also be a consequence of the

coupling between grain boundary damage processes and accommodation by dislocation creep with a pseudo-threshold stress. As the GAR increases, the accommodation process becomes increasingly more important and the material exhibits a larger fraction of the pseudo-threshold for matrix creep.

We now turn to the case in which adherence of the grain boundaries is maintained during creep, but shear stresses are relaxed by grain boundary sliding. This mechanism has orginally been invoked to explain the inferior creep strength of low-GAR grain structures.[21] Detailed modelling of the coupling between grain boundary sliding and dislocation creep[120] shows, however, that the stress concentrations resulting from sliding are quite small: the loss in creep strength due to grain boundary sliding is predicted to be only about 20%. Apart from a narrow transition region, the stress exponent of the dislocation creep process is retained down to low strain rates. The only experimental results which do not immediately contradict this prediction seem to be the creep data for dispersion strengthened aluminium measured by Rösler *et al.*[68] and Joos[67] (Fig. 11), although the material behaviour at very low strain rates is not clear. The grain boundaries in this material apparently do not contribute to premature creep fracture, which is in contrast to MA 6000. In MA 754 the strength difference between fine- and coarse-grained material (Fig. 3(b)) is, however, much higher and cannot be interpreted in terms of grain boundary sliding alone (as discussed by Nix[31]). A possible explanation for this apparent difference of the fine-grained materials may be connected with the lack of texture in MA 754 as opposed to the Al alloy which has a strong ⟨111⟩ texture.

Finally, diffusion creep can occur in fine-grained materials, which requires grain boundaries both to act as vacancy sinks and sources, and to slide. Several models have been put forward to predict the effect of grain boundary dispersoids on diffusional creep. One type of model, pioneered by Ashby[121] and detailed by Arzt *et al.*,[62] considers the emission and absorption of vacancies at the grain boundaries (the 'interface reaction') as the rate-limiting process; this idea is supported by atomistic studies of grain boundaries which suggest a fairly well-defined structure: vacancies can be produced or absorbed only at grain boundary dislocations which have to move non-conservatively in the grain boundary plane. Because these dislocations are pinned by grain boundary particles, a minimum 'threshold stress' for diffusional creep is predicted which is equal to the Orowan stress or the 'local climb' stress (eqn (9)) for boundary dislocations. Local climb is appropriate here because a boundary dislocation is constrained to remain in the boundary of the particle–matrix interface when it moves. A difficulty in

applying this model lies in the assumption that must be made with regard to the Burgers vector of the boundary dislocation; it is only clear that it is smaller than for lattice dislocations. In analogy to dislocation creep, an attractive interaction between boundary dislocations and particles could also play a role, as suggested by TEM studies of grain boundary dislocation interacting with particles.[122] But this effect has not been included in the models so far.

In another type of model it is assumed that the grain boundaries, but not the particle–matrix interfaces, act as perfect sources and sinks for vacancies. A stress concentration then builds up at the particles, which must be relaxed before creep can continue. Relaxation can occur by the nucleation of lattice dislocation loops[123] or, alternatively defect loops can be nucleated in the particle–matrix interface.[124] Both processes give rise to a 'threshold stress' for diffusion creep.

It is difficult to ascertain how important the role of diffusion creep is in the engineering alloys considered in this review. The experimental evidence for diffusion creep is limited to occasional observation of particle-free zones (e.g. Refs 40, 42). The stress dependence of the creep rate, however, is always found to be over-linear, but lower than in coarse-grained material. Such intermediate stress exponents ($n =$ 12 to 16) were reported, for example, for fine-grained dispersion strengthened aluminium alloys,[60,61] where they were attributed to interface-controlled diffusion creep with a 'threshold stress'. In order to explain the data, this 'threshold stress' must, however, be assumed to vary with applied stress, which is not predicted by theory. Another possibility would be to consider the coupling between diffusion creep and dislocation creep (with stress exponent n), as has been modelled, for example, by Greenwood *et al.*[125] In this case a stress exponent is predicted, which gradually increases from 1 to n with increasing applied stress; this also appears difficult to reconcile with experimental data.

In summary, it seems that the understanding of the behaviour of polycrystalline dispersion strengthened materials is still far from satisfactory. While some light has been shed recently on the problem of damage accumulation on grain boundaries and resulting creep fracture as a function of grain geometry, explanations for the influence of grain boundaries on the creep rate of dispersion strengthened materials have not advanced much further since the early tentative suggestions of Wilcox and Clauer.[21] From a practical point of view, coarse and elongated grains must always be considered preferable for high temperature applications, but the strength advantage over fine-grained variants seems to be material-dependent (compare, e.g., Figs 3(b) and 11). The difference in texture and the resulting types of grain

boundaries may contain a key to a better understanding of these and related effects such as the occurrence of superplasticity. Clearly further, more detailed work is necessary in these problem areas.

5 CONCLUSIONS

(1) Dispersion strengthening is an effective means of raising the temperature capability of metallic materials. Generally the creep rates are substantially reduced by the presence of dispersoid particles; the strength advantage over dispersoid-free materials is particularly pronounced at high temperatures and moderate applied stresses.

(2) From a scientific point of view, dispersion strengthened materials exhibit unusual creep behaviour, which is reflected in a high dependence of creep rates on stress and temperature. The attempts to explain the creep properties in terms of dislocation theory can be categorized into two groups, depending on whether the surmounting of the dispersoids ('climb-control') or the breaking-away from dispersoid particles ('detachment-control') is considered to be the rate-limiting event. The assumption of detachment-control, which is a new concept suggested by TEM observations, seems to have several important advantages but its validity and practical implications must still be further substantiated.

(3) From a practical point of view, the improved understanding of the mechanisms of dispersion strengthening at high temperatures may eventually contain the key to rational alloy optimization, development and use. In any case, the 'threshold stress' concept should be used with caution when laboratory data are extrapolated for design purposes. It is more likely that only an apparent 'pseudo-threshold' exists which disappears at low strain rates and/or very high temperatures. With regard to alloy design, it is concluded that besides thermodynamic stability, a dispersoid particle should have a certain optimum size and an interface to the matrix which maximizes the attractive force on dislocations. Further work will be necessary to extract practical guidelines for alloy development from these principles.

(4) The creep behaviour of polycrystalline dispersion strengthened materials is insufficiently understood. Besides producing premature creep fracture, grain boundaries also enhance the creep deformation, but the magnitude of this effect is material-dependent and is not yet predictable. Diffusion creep must be reckoned with in fine-grained materials or in elongated strain structures loaded in the transverse direction, but apparently it does not provide a satisfactory explanation for the creep of polycrystals either.

(5) Areas in which further progress would be highly desirable are the following: (i) the interaction between incoherent particles and dislocations at elevated temperatures as a function of interface structure and chemistry; and (ii) the mechanisms of creep and superplasticity in polycrystalline dispersion strengthened materials. In view of the excellent creep strength achievable in modern dispersion strengthened alloys, it should be also realized that other mechanical properties will become design-limiting, above all ductility and resistance to low and high cycle fatigue and to thermomechanical fatigue. These aspects will deserve close attention in the future.

ACKNOWLEDGEMENTS

This paper could not have been written without the numerous discussions with many colleagues over the years and without the contributions from members of my own research group, especially Drs J. Rösler, J. H. Schröder, R. Timmins and H. Zeizinger, and Mr R. Joos. I am grateful to Prof. H. Fischmeister for critically reading the manuscript and to Prof. R. F. Davis for supplying the micrograph shown in Fig. 17(c).

NOTE ADDED IN PROOF

Since submission of this manuscript in September 1988, new developments of the 'detachment model' dicussed in this paper have taken place. The new results, which have also altered the interpretation of the aluminium data described in this paper, are summarized in Ref. 112.

REFERENCES

1. Irmann, R., *Technische Rundschau* (Bern), **41** (1949) 19.
2. van Zeerleder, A., *Z. Metallkde*, **41** (1950) 228.
3. Benjamin, J. S., *Met. Trans.*, **1** (1970) 2943.
4. Singer, R. F. & Arzt, E., in *High Temperature Alloys for Gas Turbines and Other Applications 1986*, ed. W. Betz *et al.*, Dordrecht, 1986, p. 97.
5. Jangg, G. & Kutner, F., *Aluminium*, **51** (1975) 641.
6. Jangg, G., *Radex-Rundschau* (1986) 169.
7. Ansell, G. S., in *Oxide Dispersion Strengthening*, ed. G. S. Ansell, T. D. Cooper and F. V. Lenel, Gordon and Breach, New York, 1968, p. 61.
8. Ashby, M. F., in *Proc. Second Int. Conf. on Strength of Metals and Alloys*, ASM, Metals Park, Ohio, 1970, p. 507.

9. Gibeling, J. C. & Nix, W. D., *Mat. Sci. Eng.*, **45** (1980) 123.
10. Brown, L. M., in *Strength of Metals and Alloys, ICSMA 5*, ed. P. Haasen, V. Gerold & G. Kostorz, Pergamon, 1979, Vol. 3, p. 1551.
11. Brown, L. M., in *Fatigue and Creep of Composite Materials, Proc. 3rd Risø Int. Symp. on Metallurgy and Materials Science*, ed. H. Lilholt and R. Talreja, 1982, p. 1.
12. Bilde-Sørensen, J. B., in *Deformation of Multi-Phase and Particle-Containing Materials, Proc. 4th Risø Int. Symp. on Metallurgy and Materials Science*, ed. J. B. Bilde-Sørensen *et al.*, 1983, p. 1.
13. Cadek, J. & Ilschner, B., *Acta Techn. CSAV*, No. 3 (1984) 280.
14. Blum, W. & Reppich, B., in *Creep Behaviour of Crystalline Solids*, ed. B. Wilshire & R. W. Evans, Pineridge Press, Swansea, 1985, p. 83.
15. Sellars, C. M. & Petkovic-Luton, R. A., *Mat. Sci. Eng.*, **46** (1980) 75.
16. Lin, J. & Sherby, O. D., *Res Mechanica*, **2** (1981) 251.
17. Martin, J. W., *Micromechanisms in Particle-Hardened Alloys*, Cambridge University Press, Cambridge, 1980.
18. Morall, F. R., *Dispersion Strengthening of Metals*, Metals and Ceramics Information Center, Columbus, Ohio, 1977.
19. Singer, R. F. & Gessinger, G. H., in *Powder Metallurgy of Superalloys*, ed. G. H. Gessinger, Butterworth, London, 1984, p. 213.
20. Wilcox, B. A. & Clauer, A. H., *Trans. Met. Soc. AIME*, **236** (1966) 570.
21. Wilcox, B. A. & Clauer, A. H., *Acta Met.*, **20** (1972) 743.
22. Wilcox, B. A. & Clauer, A. H., in *The Superalloys*, ed. C. T. Sims and W. C. Hagel, Wiley, New York, 1972, p. 197.
23. Clauer, A. H. & Wilcox, B. A., *Met. Sci. J.*, **1** (1967) 86.
24. Kane, R. D. & Ebert, L. J., *Met. Trans.*, **7A** (1976) 133.
25. Lund, R. W. & Nix, W. D., *Acta Met.*, **24** (1976) 469.
26. Pharr, G. M. & Nix, W. D., *Scripta Met.*, **10** (1976) 1007.
27. Cairns, R. L., Curwick, L. R. & Benjamin, J. S., *Met. Trans.*, **6A** (1975) 179.
28. Howson, T. E., Stulga, J. E. & Tien, J. K., *Met. Trans.* **11A** (1980) 1599.
29. Stephens, J. J. & Nix, W. D., *Met. Trans.*, **16A** (1985) 1307.
30. Gregory, J. K., Gibeling, J. C. & Nix, W. D., *Met. Trans.*, **16A** (1985) 777.
31. Nix, W. D., *Proc. Superplastic Forming Symposium*, Los Angeles, ASM, Metals Park, Ohio, 1984.
32. Whittenberger, J. D., *Met. Trans.*, **15A** (1984) 1753.
33. Benn, R. C. & Kang, S. K., in *Superalloys 1984*, ed. M. Gell *et al.*, TMS-AIME, Warrendale, PA, 1984, p. 319.
34. Singer, R. F. & Gessinger, G. H., *Met. Trans.*, **13A** (1982) 1463.
35. Arzt, E. & Singer, R. F., in *Superalloys 84*, ed. M. Gell *et al.*, TMS-AIME, Warrendale, PA, 1984, p. 367.
36. Zeizinger H. & Arzt, E., *Z. Metallkde*, **79** (1988) 774.
37. Arzt, E., Elzey, D. & Schröder, J., in *Advanced Materials and Processing Techniques for Structural Applications*, ed. T. Khan and A. Lasalmonie, ASM Europe Technical Conference, ONERA, Chatillon, 1987, p. 327.
38. Elzey, D. M. & Arzt, E., in *Superalloys*, ed. S. Reichman *et al.*, TMS, 1988, pp. 595.
39. Incomap, Data Sheet, 1983.
40. Timmins, R. & Arzt, E., *Scripta Met.*, **22** (1988) 1353.

41. Whittenberger, J. D., *Met. Trans.*, **4** (1973) 1475.
42. Whittenberger, J. D., *Met. Trans.*, **8A** (1977) 1155.
43. Sautter, F. K. & Chen, E. S., in *Oxide Dispersion Strengthening, Proc. 2nd Bolton Landing Conf.*, Gordon and Breach, New York, 1969, p. 495.
44. Burton, B., *Metal Sci. J.*, **5** (1971) 11.
45. Burton, B. & Beere, W. B., *Met. Sci.*, **12** (1978) 71.
46. Clegg, W. J. & Martin, J. W., *Met. Sci.*, **16** (1982) 65.
47. Crossland, I. G. & Clay, B. D., *Acta Met.*, **25** (1977) 929.
48. Nilsson, J.-O., Howell, P. R. & Dunlop, G. L., *Acta, Met.*, **27** (1979) 179.
49. Sritharan, T. & Jones, H., *Acta Met.*, **28** (1980) 1633.
50. Sritharan, T. & Jones, H., *Met. Sci.*, **15** (1981) 365.
51. Shepherd, C. M., James, A. W. & Titchmarsh, J. M., Report AERE-R 11322, UKA EA Harwell, Harwell, UK, 1985.
52. Sinha, R. K. & Blachere, J. R., *Scripta Met.*, **13** (1979) 41.
53. Clegg, W. J., *Scripta Met.*, **18** (1984) 767.
54. Ansell, G. S. & Weertman, J., *Trans. Met. Soc. AIME*, **215** (1959) 838.
55. Milicka, K., Cadek, J. & Rys, P., *Acta Met.*, **18** (1970) 733.
56. Cadek, J., *Czech. J. Phys.*, **B31** (1981) 177.
57. Clauer, A. H. & Hansen, N. *Acta Met.*, **32** (1984) 269.
58. Oliver, W. C. & Nix, W. D., *Acta Met.*, **30** (1982) 1335.
59. Otsuka, M., Abe, Y. & Horiuchi, R., in *Creep and Fracture of Engineering Materials and Structures*, ed. B. Wilshire and R. W. Evans, The Institute of Metals, London, p. 307.
60. Orlova, A., Kucharova, K. & Cadek, J., unpublished research, 1988.
61. Kucharova, K., Orlova, A., Oikawa, H. & Cadek, J., *Mat. Sci. Eng.*, in press.
62. Arzt, E., Ashby, M. F. & Verrall, R. A., *Acta Met.*, **31** (1983) 1977.
63. Nieh, T. G., Gilman, P. S. & Wadsworth, J., *Scripta Met.*, **19** (1985) 1375.
64. Matsuda, N. & Matsuura, K., *Trans. Jap. Inst. Met.*, **28** (1987) 392.
65. Arzt, E. & Rösler, J., in *Dispersion Strengthened Aluminium Alloys*, ed. Y.-W. Kim and W. M. Griffith, TMS, 1988, p. 31.
66. Rösler, J., PhD Thesis, University of Stuttgart, 1988.
67. Joos, R., Diploma Thesis, University of Stuttgart, 1988 and Arzt, E. & Joos, R., *Scripta Met.*, **23** (1989) 1595.
68. Rösler, J., Joos, R. & Arzt, E., to be published.
69. Slesar, M., Besterci, J., Jangg, G., Miskovicova, M. & Pelikan, K., *Z. Metallkde*, **79** (1988) 56.
70. Olsen, R. J. & Ansell, G. S., *Trans. ASM*, **62** (1969) 711.
71. Yaney, D. L., Öveçoglu, M. L. & Nix, W. D., in *Dispersion Strengthened Aluminium Alloys*, ed. Y.-W. Kim and W. M. Griffith, TMS, 1988, p. 619.
72. Pharr, G. M., Zedalis, M. S., Skinner, D. J. & Gilman, P. S., in *Dispersion Strengthened Aluminium Alloys*, ed. Y.-W. Kim and W. M. Griffith, TMS, 1988, p. 309.
73. Petkovic-Luton, R., Srolovitz, D. J. & Luton, M. J., in *Frontiers of High Temperature Materials II*, ed. J. S. Benjamin and R. C. Benn, INCO Alloys International, New York, p. 73.
74. Peterseim, J. & Sauthoff, G., *Steel Res.*, **56** (1985) 483.
75. Peterseim, J. & Sauthoff, G., Steel Res., **57** (1986) 19.
76. Pugh, J. W., *Met. Trans.* **4** (1973) 533.

77. Wright, P. K., *Met. Trans.*, **9A** (1978) 955.
78. Mukherjee, A. K., Bird, J. E. & Dorn, J. E., *Trans. ASM*, **62** (1969) 155.
79. Barrett, C. R., Ardell, A. J. & Sherby, O. D., *Trans. AIME*, **230** (1964) 200.
80. Malu, M. & Tien, J. K., *Scripta Met.* **9** (1975) 1117.
81. Barrett, C. R., *Trans. AIME*, **239** (1967) 1726.
82. Gittus, J. H., *Proc. Roy. Soc. Lond.*, **A342** (1975) 279.
83. Reppich, B., Listl, W. & Meyer, T., in *High Temperature Alloy for Gas Turbines and Other Applications 1986*, ed. W. Betz *et al.*, Reidel, Dordrecht, 1986, p. 1023.
84. Guyot, P., *Acta Met.*, **12** (1964) 941.
85. Ansell, G. S. & Lenel, F. V., *Trans. TMS–AIME*, **221** (1961) 452.
86. Holbrook, J. H. & Nix, W. D., *Met. Trans.*, **5** (1973) 1033.
87. Brown, L. M. & Ham, R. K., in *Strengthening Methods in Crystals*, ed. A. Kelly and R. B. Nicholson, Elsevier, Amsterdam, 1971, p. 9.
88. Shewfelt, R. S. W. & Brown, L. M., *Phil. Mag.*, **30** (1974) 1135, **35** (1977) 945.
89. Evans, H. E. & Knowles, G., *Met. Sci.*, **14** (1980) 262.
90. McLean, M., Acta Met., **33** (1985) 545.
91. Arzt, E., unpublished results, 1988.
92. Arzt, E. & Ashby, M. F., *Scripta Met.*, **16** (1982) 1285.
93. Humphreys, F. J., Hirsch, P. B. & Gould, D., in *Proc. Second Int. Conf. on Strength of Metals and Alloys*, ASM, Metals Park, Ohio, 1970, p. 550.
94. Lagneborg, R., *Scripta Met.*, **7** (1973) 605.
95. Hausselt, J. H. & Nix, W. D., *Acta Met.*, **25** (1977) 1491.
96. Rösler, J. & Arzt, E., *Acta Met.*, **36** (1988) 1043.
97. Nardone, V. C. & Tien, J. K., *Scripta Met.*, **17** (1983) 467.
98. Schröder, J. H. & Arzt, E., *Scripta Met.*, **19** (1985) 1129.
99. Arzt, E. & Schröder, J. H., in *High Temperature Alloys for Gas Turbines and Other Applications 1986*, ed. W. Betz *et al.*, Reidel, Dordrecht, 1986, p. 1037.
100. Schröder, J. H., Doctoral Dissertation, University of Stuttgart, 1987.
101. Davis, R. F. & Posthill, J. B., private communication, 1987.
102. Cassada, W. A., Shiflet, G. J. & Starke Jr, E. A., *Acta Met.*, **34** (1986) 367.
103. Srolovitz, D. J., Petkovic-Luton, R. & Luton, M. J., *Scripta Met.*, **16** (1982) 1401.
104. Srolovitz, D. J., Petkovic-Luton, R. & Luton, M. J., *Phil. Mag.*, **48** (1983) 795.
105. Srolovitz, D. J., Petkovic-Luton, R. & Luton, M. J., *Acta Met.*, **31** (1983) 2151.
106. Srolovitz, D. J., Luton, M. J., Petkovic-Luton, R., Barnett, D. M. & Nix, W. D., *Acta Met.*, **32** (1984) 1079.
107. Mori, T., Okabe, M. & Mura, T., *Acta Met.* **28** (1978) 319.
108. Weeks, R. W., Pati, S. R., Ashby, M. F. & Barrand, P., *Acta Met.*, **17** (1969) 1403.
109. Arzt, E. & Wilkinson, D. S., *Acta Met.*, **34** (1986) 1893.
110. Russell, K. C. & Brown, L. M., *Acta Met.*, **20** (1972) 969.
111. Arzt, E. & Rösler, J., *Acta Met.*, **36** (1988) 1053.

112. Rösler, J. & Arzt, E., *Acta Met.*, **38** (1990) 671.
113. Benjamin, J. S., Discussion contribution in *Frontiers of High Temperature Materials II*, ed. J. S. Benjamin and R. C. Benn, INCO Alloys International, New York, 1983, p. 120.
114. Ashby, M. F., *Acta Met.*, **14** (1966) 679.
115. Bacon, D. J., Kocks, U. F. & Scattergood, R. O., *Phil. Mag.* **28** (1973) 1241.
116. Hausselt, J. H. & Nix, W. D., *Acta Met.*, **25** (1977) 595.
117. Arzt, E., *Z. Metallkde*, **75** (1984) 206.
118. Stephens, J. J. & Nix, W. D., *Met. Trans.*, **17A** (1986) 281.
119. Cocks, A. C. F. & Ashby, M. F., *Progr. Mat. Sci.*, **27** (1982) 189.
120. Crossman, F. W. & Ashby, M. F., *Acta Met.*, **23** (1975) 425.
121. Ashby, M. F., *Scripta Met.*, **3** (1969) 837.
122. Dunlop, G. L., Nilsson, J.-O. & Howell, P. R., *J. Microscopy*, **116** (1979) 115.
123. Harris, J. E., *Met. Sci. J.*, **7** (1973) 1.
124. Burton, B., *Mat. Sci. Eng.*, **11** (1973). 337.
125. Greenwood, G. W., Jones, H. & Sritharan, T., *Phil. Mag.* **A41** (1980) 871.
126. Wilcox, B. A., Clauer, A. H. & Hutchinson, W. B., NASA—Report CR 72832, 1971.
127. Servi, I. S. & Grant, N. J., *Trans. AIME*, **3** (1951) 917.